NASA/TM—2013-216501

Large Scale Flame Spread Environmental Characterization Testing

Lauren K. Clayman, Sandra L. Olson, Suleyman A. Gokoglu, and John E. Brooker
Glenn Research Center, Cleveland, Ohio

Paul V. Ferkul
National Center for Space Exploration, Glenn Research Center, Cleveland, Ohio

Henry F. Kacher
Glenn Research Center, Cleveland, Ohio

April 2013

NASA STI Program . . . in Profile

Since its founding, NASA has been dedicated to the advancement of aeronautics and space science. The NASA Scientific and Technical Information (STI) program plays a key part in helping NASA maintain this important role.

The NASA STI Program operates under the auspices of the Agency Chief Information Officer. It collects, organizes, provides for archiving, and disseminates NASA's STI. The NASA STI program provides access to the NASA Aeronautics and Space Database and its public interface, the NASA Technical Reports Server, thus providing one of the largest collections of aeronautical and space science STI in the world. Results are published in both non-NASA channels and by NASA in the NASA STI Report Series, which includes the following report types:

- TECHNICAL PUBLICATION. Reports of completed research or a major significant phase of research that present the results of NASA programs and include extensive data or theoretical analysis. Includes compilations of significant scientific and technical data and information deemed to be of continuing reference value. NASA counterpart of peer-reviewed formal professional papers but has less stringent limitations on manuscript length and extent of graphic presentations.

- TECHNICAL MEMORANDUM. Scientific and technical findings that are preliminary or of specialized interest, e.g., quick release reports, working papers, and bibliographies that contain minimal annotation. Does not contain extensive analysis.

- CONTRACTOR REPORT. Scientific and technical findings by NASA-sponsored contractors and grantees.

- CONFERENCE PUBLICATION. Collected papers from scientific and technical conferences, symposia, seminars, or other meetings sponsored or cosponsored by NASA.

- SPECIAL PUBLICATION. Scientific, technical, or historical information from NASA programs, projects, and missions, often concerned with subjects having substantial public interest.

- TECHNICAL TRANSLATION. English-language translations of foreign scientific and technical material pertinent to NASA's mission.

Specialized services also include creating custom thesauri, building customized databases, organizing and publishing research results.

For more information about the NASA STI program, see the following:

- Access the NASA STI program home page at *http://www.sti.nasa.gov*

- E-mail your question to *help@sti.nasa.gov*

- Fax your question to the NASA STI Information Desk at 443–757–5803

- Phone the NASA STI Information Desk at 443–757–5802

- Write to:
  STI Information Desk
  NASA Center for AeroSpace Information
  7115 Standard Drive
  Hanover, MD 21076–1320

NASA/TM—2013-216501

Large Scale Flame Spread Environmental Characterization Testing

Lauren K. Clayman, Sandra L. Olson, Suleyman A. Gokoglu, and John E. Brooker
Glenn Research Center, Cleveland, Ohio

Paul V. Ferkul
National Center for Space Exploration, Glenn Research Center, Cleveland, Ohio

Henry F. Kacher
Glenn Research Center, Cleveland, Ohio

National Aeronautics and
Space Administration

Glenn Research Center
Cleveland, Ohio 44135

April 2013

Acknowledgments

This work was funded by the Spacecraft Fire Safety Demonstration Project under the Advanced Exploration Systems Program. The authors would like to thank the Project Manager, Gary Ruff and the Principal Investigator, David Urban for their management and guidance. The authors would also like to thank Michael Johnston for his assistance with test planning and preparation and Justin Niehaus for his data analysis support. Finally, the authors extend thanks to the rest of the test team, including the facility engineers and technicians, who all made significant contributions toward test preparation and execution.

Level of Review: This material has been technically reviewed by technical management.

Available from

NASA Center for Aerospace Information
7115 Standard Drive
Hanover, MD 21076–1320

National Technical Information Service
5301 Shawnee Road
Alexandria, VA 22312

Available electronically at http://www.sti.nasa.gov

Contents

List of Tables

List of Figures

Large Scale Flame Spread Environmental Characterization Testing

Lauren K. Clayman, Sandra L. Olson, Suleyman A. Gokoglu, and John E. Brooker
National Aeronautics and Space Administration
Glenn Research Center
Cleveland, Ohio 44135

Paul V. Ferkul
National Center for Space Exploration Research
Glenn Research Center
Cleveland, Ohio 44135

Henry F. Kacher
National Aeronautics and Space Administration
Glenn Research Center
Cleveland, Ohio 44135

Abstract

Under the Advanced Exploration Systems (AES) Spacecraft Fire Safety Demonstration Project (SFSDP), as a risk mitigation activity in support of the development of a large-scale fire demonstration experiment in microgravity, flame-spread tests were conducted in normal gravity on thin, cellulose-based fuels in a sealed chamber. The primary objective of the tests was to measure pressure rise in a chamber as sample material, burning direction (upward/downward), total heat release, heat release rate, and heat loss mechanisms were varied between tests. A Design of Experiments (DOE) method was imposed to produce an array of tests from a fixed set of constraints and a coupled response model was developed. Supplementary tests were run without experimental design to additionally vary select parameters such as initial chamber pressure. The starting chamber pressure for each test was set below atmospheric to prevent chamber overpressure. Bottom ignition, or upward propagating burns, produced rapid acceleratory turbulent flame spread. Pressure rise in the chamber increases as the amount of fuel burned increases mainly because of the larger amount of heat generation and, to a much smaller extent, due to the increase in gaseous number of moles. Top ignition, or downward propagating burns, produced a steady flame spread with a very small flat flame across the burning edge. Steady-state pressure is achieved during downward flame spread as the pressure rises and plateaus. This indicates that the heat generation by the flame matches the heat loss to surroundings during the longer, slower downward burns. One heat loss mechanism included mounting a heat exchanger directly above the burning sample in the path of the plume to act as a heat sink and more efficiently dissipate the heat due to the combustion event. This proved an effective means for chamber overpressure mitigation for those tests producing the most total heat release and thusly was determined to be a feasible mitigation strategy to incorporate into the microgravity experiment.

1.0 Introduction

Past and present space programs have emphasized the need to address practical spacecraft fire safety issues for crewed vehicles on exploration missions. As part of the Advanced Exploration Systems (AES) Program, the Spacecraft Fire Safety Demonstration Project (SFSDP) was initiated to develop technology in all areas of fire safety. While many experiments have been performed on small scale samples as a way to understand the basic science of combustion and flammability, characterizing fires that are more substantial in size has not been executed in a controlled space environment. The project has proposed a zero-gravity large-scale fire demonstration experiment to reveal material flammability, burning trends, and environmental (control volume) impacts. In addition, experimental data will allow for the verification of detailed numerical models of such an event. Many material tests have been conducted in microgravity to characterize combustion and flammability characteristics, but experiments to date have not been considered large-scale. Among the tasks developed in support of the SFSDP large-scale spaceflight experiment, is the initiative to understand and characterize the environmental impact of such an event to a spacecraft. A major safety concern for any carrier vehicle is the environmental effect of a large-scale burn. As a risk mitigation activity supporting environmental characterization, a full-scale fire demonstration experiment was conducted in vacuum chamber at the NASA Glenn Research Center (GRC).

Similar material burning experiments have been conducted at GRC, but with different objectives. The primary objective of this test was to measure pressure rise in a large sealed chamber and to characterize that data as a function of sample material, burning direction (upward/downward), heat release rate, total heat release, and heat loss mechanisms. Unlike tests before it, this task did not intend to examine the burning phenomena of various fuel materials, but rather the changes to the ambient environment. The experimental data will lend itself to producing useful correlations and trends, answering engineering and design unknowns, and providing an anchor upon which to validate analytical models. Data gathered from this test will serve as risk mitigation in terms of facilitating further definition of the expected environment that will result from burning candidate flight material in a closed volume. The experimental outcomes will fold into the project's Safety Data Package.

1.1 Purpose

The purpose of this test report is to provide a description of the experimental test set up and associated hardware and equipment, to provide a synopsis of the test procedure, and to provide examples of data instrumentation plots to facilitate data interpretation.

2.0 Facility

Vacuum Facility 13 (VF-13), is a large volume chamber residing in building 301 designed for tests requiring a high vacuum environment (Fig. 1). This test utilized the chamber to provide a reduced pressure environment. It has a 149.9 cm inner diameter, and a height of 360 cm, yielding a total volume of 6.35 m^3. The base is 107.9 cm deep and supports the electrical feed-throughs. It has a removable steel

Figure 1.—Vacuum Facility 13.

cap that is 252.1 cm tall. The cap has four viewing windows. It attaches to the base via connecting flanges. An experimental rack was fabricated to fit into the chamber to support the integration of the test components and will be detailed in the experimental hardware description.

3.0 Test Description

By varying constraints such as heat loss mechanisms and sample burning rate, experimental outputs will more effectively validate analytical simulations. To achieve these variations, the experiment was designed to accommodate a removable quenching mechanism at the sample mounting location, as well as the addition of a thermal mass, or heat exchanger, downstream of the burn plume to more closely mimic the expected flight configuration. Sample holders (also referred to as fuel cards) were designed to accommodate different material sizes and were wired such that ignition could be achieved at either the top or bottom of a sample. The material burning rate was varied between tests by burning the material samples either simultaneously or sequentially and by varying ignition location to mimic possible flight experiment burning scenarios and to help provide a range of data for analytical simulation validation.

For each test, VF-13 was sealed and the air inside was evacuated until reaching a specified starting test pressure. Up to two runs were performed during each test. A mixing fan was mounted to the bottom of the experimental rack to mix the chamber air after each test to help encourage chamber equilibrium. Upon test completion, the chamber air was partially evacuated and then refilled to vent the combustion products before removing the chamber lid. The comprehensive operational test procedure is included in Appendix A.

As described further in section 3.1, experimental instrumentation for data collection included a pressure transducer for measuring tank pressure, thermocouples for capturing tank air temperature, radiometers for estimating radiant heat flux, anemometers to measure air flow, and video cameras for visually documenting the material burning rate. Feed-throughs were needed for the experimental data instrumentation, the ignition system, and the camera system (including the LED strips described in the Cameras section). Figure 2 is a photograph of the experimental rack, hardware, and instrumentation. Appendix B details the XYZ coordinate locations for the instrumentation.

Given the wide-ranging objectives of this test, a controlled approach was taken to yield a set of tests that would best produce meaningful data correlations. Using a Design of Experiments (DOE) method, an array of tests was produced using a fixed set of parametric constraints. A supplementary set of tests was run which included a second sample material and several additionally varied parameters that deviated from the DOE constraints. Both test matrices are included in Appendix C. In this document any test cases referred to by test/fill and run number are prefixed with either DOE, identifying the tests in the Design of Experiments matrix, or SUP, identifying the tests in the Supplementary test matrix.

3.1 Experimental Rack, Hardware, and Instrumentation

3.1.1 Frame

A frame was constructed to fit within VF-13 that sits on an inner rim at the connecting flanges shown in Figures 1 and 2. The frame is made of Bosch Rexroth aluminum structural framing. It is capable of supporting one sample holder at a time. The sample holders are described in more detail in the following section. The frame supports Lexan (SABIC Innovative Plastics) glass panels which surround the sample holder on all four sides, partially mimicking the expected flight design enclosure configuration by acting as a combustion tunnel. Figure 2 illustrates the entire test rig. The original experimental concept sketch can be found in Appendix D, and dimensioned drawings are included in Appendix B.

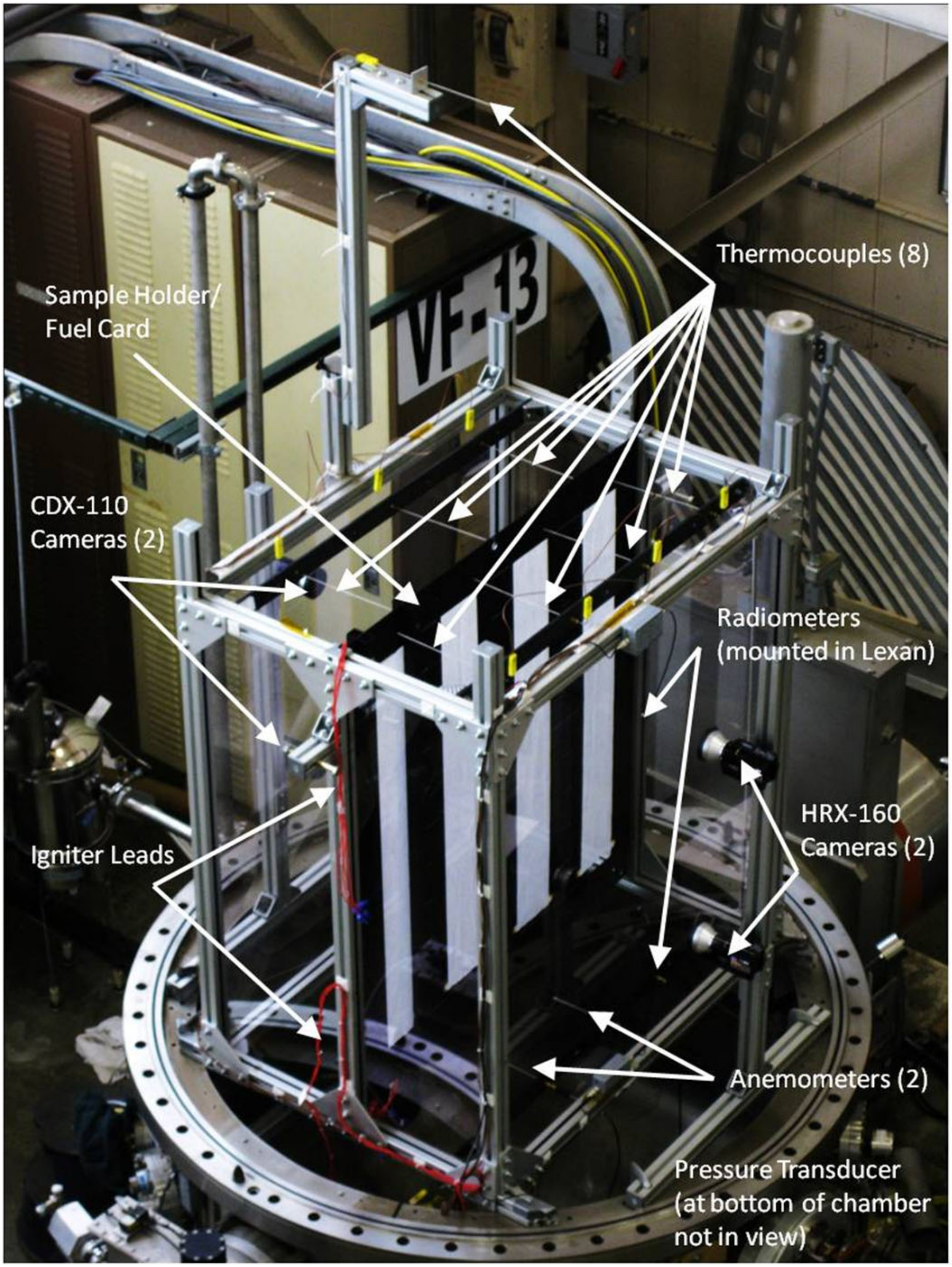

Figure 2.—Experimental rack in VF-13.

3.1.2 Sample Holder

As mentioned, an objective of the test was to vary heat release rate. This was achieved by varying the sample width and burning multiple samples sequentially while keeping the total sample area constant. Three sample holder designs were conceived for testing. Drawings were produced for the three sample holder designs and were submitted to GRC Manufacturing Division for fabrication. The dimensioned drawings can be found in Appendix E. Manufacturing ordered the material (1/16 in. thick aluminum), and cut the sample holders using a water knife. Due to the effort to constrain the input variables for the DOE matrix generation, only the four slot sample holder was used for DOE testing. The four slot sample holder and the one slot sample holder were both used for supplemental testing. The three slot sample holder was fabricated but never utilized. Figure 3 shows a depiction of the three designs. The two designs used during the test are shown in bold.

To reduce the potential for reflection on the video recordings, the sample holders were sent offsite for flat black anodizing. Two of each sample holder design were fabricated (for a total of six sample holders) with the intent of expediting test preparations. The sample holders were not permanently mounted as part of the test fixture, but were designed to be easily installed and removed between tests. Because of the size of the sample holders and the height of the facility and test rig, the sample holders needed to be installed and removed using the facility crane. Procedures for sample holder installation and removal are included in Appendix F and Appendix G, respectively.

Each sample holder was designed with the capability of igniting at either end of the sample. Igniter wires were permanently affixed to each end of the sample holders (Figs. 2 and 4). Graduation lines (scale factors) were drawn alongside the vertical perimeters of the sample cutouts to facilitate tracking the burn rate. Kapton tape was used to mount the samples to the sample holder.

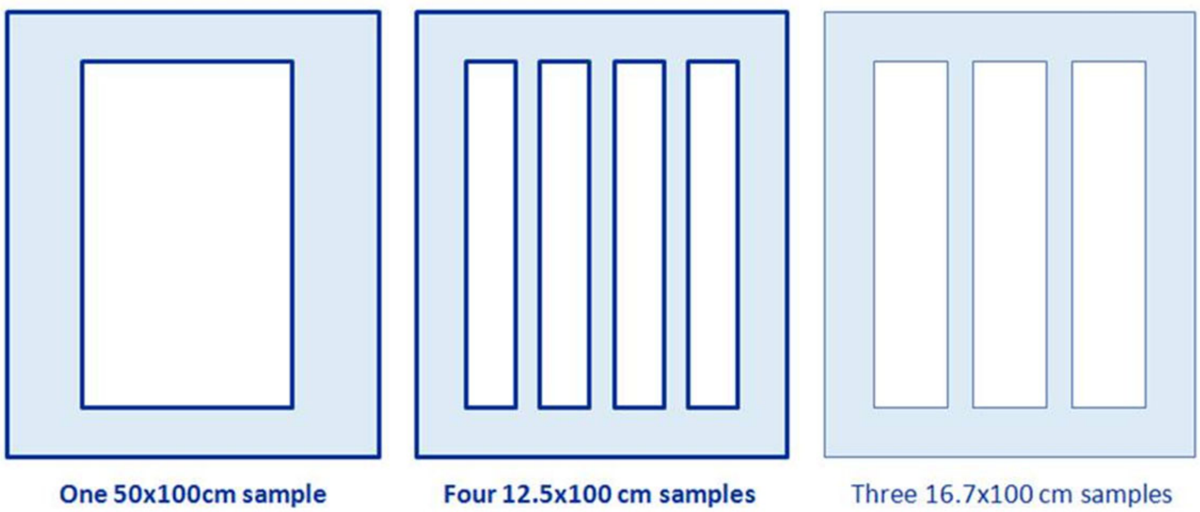

Figure 3.—Depiction of sample holder designs (not to scale).

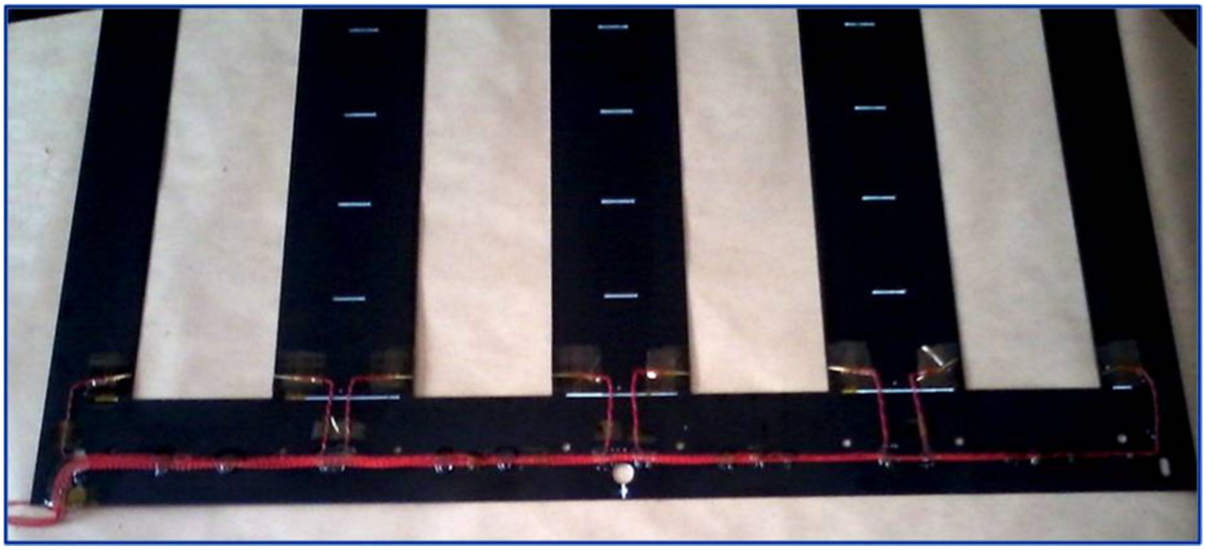

Figure 4.—Igniter wiring leads on a four slot sample holder.

3.1.3 Cameras

For this test, the four chamber viewing ports did not provide access for visual documentation of the experiment. Four HD digital video cameras, two mounted on either side of the sample holder, recorded and transmitted video of the experiment inside the chamber. Two of the cameras were purchased new (mounted in the front) and two cameras were borrowed. Wide angle lenses were purchased for both sets of cameras as the fields of view did not completely cover the entire sample area. With the addition of the lenses, the front cameras captured the entire potential sample area, while the back cameras did not. The camera locations are labeled in Figure 2 and additional information pertaining to the cameras can be found in and Appendix B.

The cameras were mounted outside of the Lexan enclosure. Aside from documenting the experiments, the primary intent of the video imaging was to post-process the videos to reveal the burning rate of the samples. Secondarily, a live video feed was transmitted from the two front cameras to two flat screen monitors provided test operators with visual confirmation of fuel sample ignition and the outcome of the test. Illumination within the chamber to facilitate adequate lighting for video imagery was achieved with a series of green Light Emitting Diode (LED) strips, which were mounted vertically inside along the two front corners of the Bosch frame. More information pertaining to the LED strips can be found in Table 1.

The cameras were not configured to operate remotely. As a result, the cameras needed to be turned on and recording prior to closing the chamber. Video data captured by the cameras was written to Secure Digital (SD) cards. During the course of testing, reflections were hindering flame tracking post-processing of the video data files. A thin sheet of black card stock was added to the inner surface of the back Lexan panel to help minimize the reflection for the front set of cameras. All camera settings are captured in Appendix H.

3.1.4 Thermocouples

The facility had existing feed-throughs capable of supporting eight type K thermocouples. All eight were utilized for testing. Seven thermocouples were mounted in the plane directly above the top edge of the sample holder, with four evenly spaced on the front side and three evenly spaced on the back side of the test rig. The spacing was intended to allow for capturing temperature readings directly above the center of the sample being burned, despite which sample holder was being used. An eighth thermocouple was mounted one meter above the top edge of the sample holder to obtain a plume temperature reading. Thermocouple information can be found in Table 1.

TABLE 1.—EXPERIMENTAL INSTRUMENTATION

Description	Manufacturer/Model number	Quantity	Serial number	Comments
Thermocouple	Omega, KMQSS-062(E)-12	8	NA	
Radiometer (Thermopile Detectors)	ORIEL instruments, 7108	2	NA	Utilized two amplifiers, one for each radiometer (supplier, Dexter Research Center, Model 1010 Low Noise Amplifier)
Anemometer	TSI, 8475-12	2	62010041, 02/28/2012; 62010042, 02/24/2012	
Camera	SONY HDR-XR160 HD (2) SONY HDR-CX110 (2)	4	HDR-XR160 1179957-P 1179960-J HDR-CX160 1197443-F 1202996-F	Wide angle lenses were purchased for the cameras (SONY VCL-HA07A wide angle adaptor, QTY 4)
Pressure transducers	Setra 205-2 Setra 270	1	Setra 205-2, 530528; Setra 270, N/A	Setra 205-2 had a range of 0 to 25 psia and an accuracy of ±0.11% FS. Setra 270 had a range of 0 to 20 psia and an accuracy of ±0.05% FS.
LED strips	RL-SC-RSM-G-10	1	N/A	
Kanthal igniter wire	Product: Kanthal A-1 Size (diameter): 0.0113 in. B&S wire gauge: 29 T: 0.45 Ω/FT: 6.751 Net: 0.73 REF NO.: 50130	N/A	N/A	For sawtooth/sinusoid shaped igniters, actual wire lengths were approximately double igniter length.

The thermocouple arrangement was revised for tests which utilized a heat exchanger. The thermocouple diagrams documenting the progression of the thermocouple arrangement are in Appendix I. Figure 2 shows the thermocouples on the test rig. Appendix B includes XYZ coordinates for the thermocouples. A thermocouple support plate was designed with pre-drilled holes to facilitate thermocouple mounting. Three support plates were fabricated by manufacturing and also sent out for flat black anodizing. Two of the support plates were used for thermocouple mounting, while the third and spare plate was instead used to mount the anemometers. The drawing for the thermocouple support plate is included in Appendix E.

3.1.5 Radiometers

Mounted within the front panel of Lexan were two radiometers for detecting radiant flux. Both were aligned vertically along the center of the Lexan panel. Two amplifiers were used for the radiometers. Table 1 lists additional radiometer information. Figure 2 points out the location of the radiometers on the test rig and their XYZ coordinates can be found in Appendix B.

3.1.6 Anemometers

Measuring induced buoyant flow was of interest for this test. Two omnidirectional anemometers were mounted several inches away from the base of the sample holder plane. Table 1 lists additional anemometer information. The anemometers are labeled in Figure 2 and actual XYZ coordinates are called out in Appendix B. A thermocouple support plate was used for mounting the anemometers. The drawing for the thermocouple support plate is included in Appendix E. The anemometer test data readings appeared to saturate at approximately 55 cm/s. Airflows of this magnitude were only present while the mixing fan was operational.

3.1.7 Pressure Transducers

Two pressure transducers were actively recording data during testing. One pressure transducer was left in the facility by the previous occupant and had expired calibration certification. It measured pressures within a range of 0 to 20 psi. The second pressure transducer was calibrated prior to testing and it had a range of
0 to 25 psi. While both pressure transducer readings are present in the test data, only the 0 to 25 psi range pressure transducer data is being considered for post-test evaluation and data correlations. The make and model of these transducers are included in Table 1. The pressure transducers were mounted in the chamber feed-throughs (at the chamber wall) approximately 1 ft below the bottom of the test rig. The 0 to 25 psi range transducer mounted in the feed-through near the front left corner of the test rig and the 0 to 20 psi transducer was mounted in the feed-through near the front right corner of the test rig.

3.1.8 Mixing Fan

To aid in mixing the chamber air following test runs, a fan was mounted along the base of the frame. Fan mounting location and air flow direction were not of concern, provided the fan did not interfere with the test article.

3.1.9 Igniters

Kanthal wire was used to create the igniters used for each test. More information regarding the Kanthal wire can be found in Table 1. For the majority of the tests the wire was bent in sinusoid/sawtooth shape until the total length of the igniter was the width of the test sample. Connector pins were crimped onto the ends. See Figures 4 to 6. The sawtooth shape of the igniter lent itself well to attaching to the sample by alternating peaks above and below the edge of the sample. The igniters were reused until broken, distorted beyond repair, or too brittle.

Concerned that the wire would become hot and sag too quickly, for large sample (50 by 100 cm) tests, the igniter wire was simply woven through the fabric like a thread rather than attaching to the sample by weaving alternating peaks around the edge. The igniters were supplied with a constant current just under 4 A (approximately 3.9 A). The voltage source was an 84 V DC source, but the voltage drawn was variable depending on igniter resistance (igniter length).

A switchbox was custom made for the experiment. It allowed for the experiments four igniters to be engaged in any combination, either simultaneously or sequentially, and it also allowed for synchronization of the illumination of the LED lights with ignition.

Figure 5.—Igniter concept.

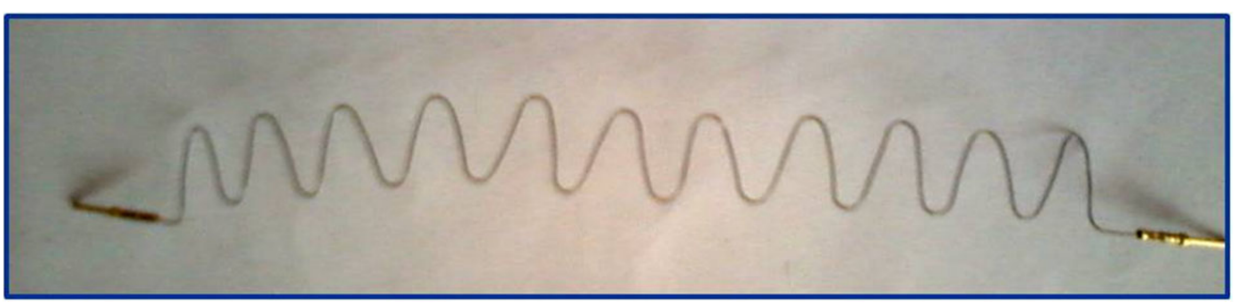

Figure 6.—Photo of igniter.

3.1.10 Heat Exchangers

As a means of varying heat loss during testing, two different heat absorbing panel configurations were used. These were both referred to as heat exchangers. The heat exchangers needed to be porous so as not to obstruct the induced buoyant flow during burning.

The first configuration was comprised of two stacked aluminum honeycomb core panels from McMaster Carr. Each was 24 in. wide by 48 in. long by 0.5 in. thick with 0.5 in. cells. The aluminum itself was approximately 2 mils thick (a measured value upon receipt of the product from the manufacturer). Figure 7 shows a depiction of an aluminum honeycomb core similar to what was used for this test.

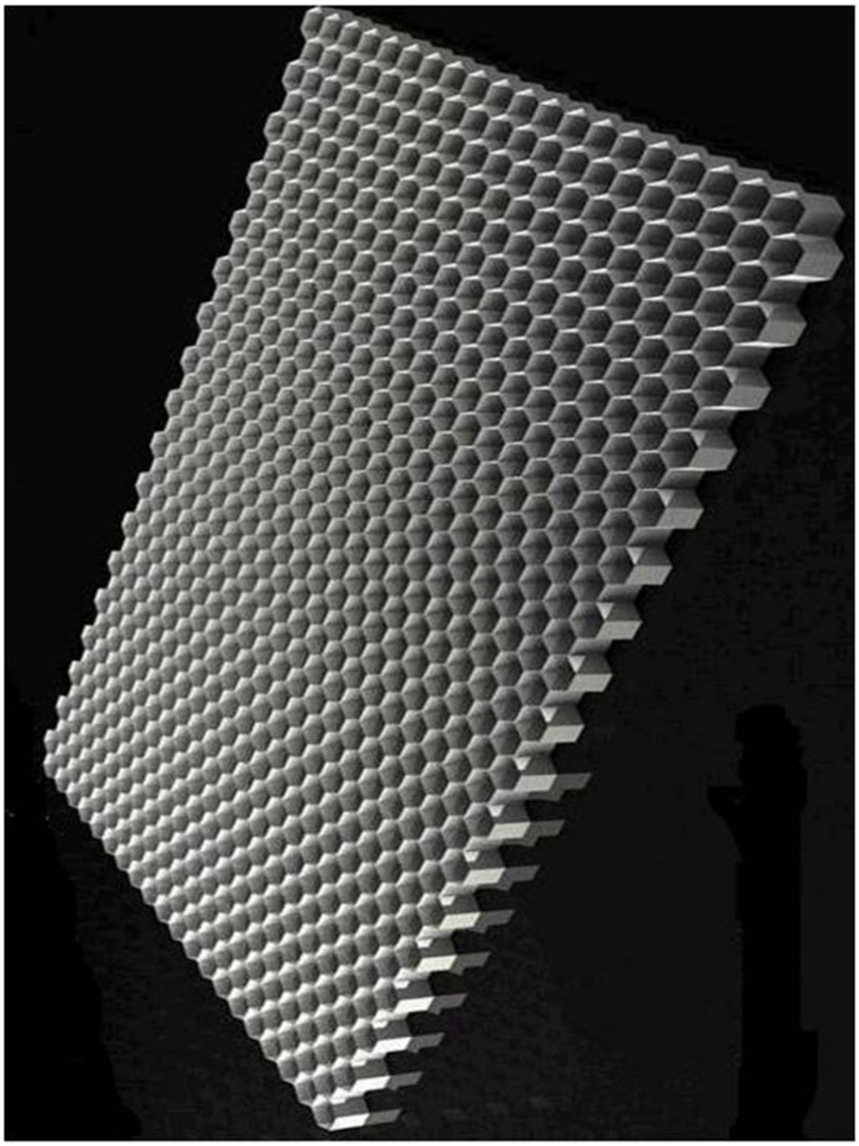

Figure 7.—Depiction of an aluminum honeycomb core (similar to L1).

The two panels were stacked together so that the cells were slightly offset and simply placed across the top of the test frame. The length of the panels exceeded the length of the frame so they protruded slightly on either side. The panel width was slightly less than the width of the frame so a ceramic paper was cut into long strips and used to eliminate the gap. The two panels together weighed 770 g (one weighed 380 g, one weighed 390 g). When the honeycomb began to lose its rigidity, it became evident that the honeycomb was bonded with adhesive and was not welded. This heat exchanger is referred to as “L1” within the context of the test matrices. The reference was an arbitrary label for the purposes of providing nomenclature for the parametric input to the DOE software.

The second heat exchanger was comprised of two aluminum mesh (lath) panels with an aluminum frame from filters-now.com. The frame dimensions were 24 in. wide by 43 in. long by 7/8 in. thick. The mesh was 5/8 in. and was secured by the frame. Figure 8 is a photograph of one of the two panels. The two panels were stacked together and placed across the top of the experimental frame during testing. Unlike the honeycomb panels, the length of the mesh panels did not exceed the experimental frame length, however the panel width was slightly less than the width of the experimental frame so a ceramic paper was cut into long strips and used to eliminate the gap.

Figure 8.—Photo of one of two aluminum mesh heat exchanger panels (L2).

The two panels together weighed 5208 g (one weighed 2610 g, one weighed 2598 g). No adhesives were used in the fabrication of these panels. However, while testing, it became evident that the mesh had an undisclosed protective coating. Mesh panels with coatings are not uncommon given their range of applicability; microwaves, stove hoods, etc. The coating caused excess smoke release during several of the tests and at least once caused a secondary burn to occur as the coating caught on fire from the heat and intensity of the burning sample. This heat exchanger is referred to as “L2” within the context of the test matrices.

3.1.11 Quench Bars

As a secondary means of varying heat loss, aluminum bars, called quench bars, were designed to fasten along the vertical perimeters of samples on both the front and back of the sample holders. This means that four quench bars would be attached per sample. Figure 9 illustrates a depiction of a sample card with quench bars. The bars were made of 0.0625 in. thick aluminum and were each 43.25 in. long with a 1 in. square hollow cross section. Each bar was painted black with off the shelf spray paint to help minimize reflection from both the LED lights and the flame from the burning sample. The bars bolted to the sample holder at each end.

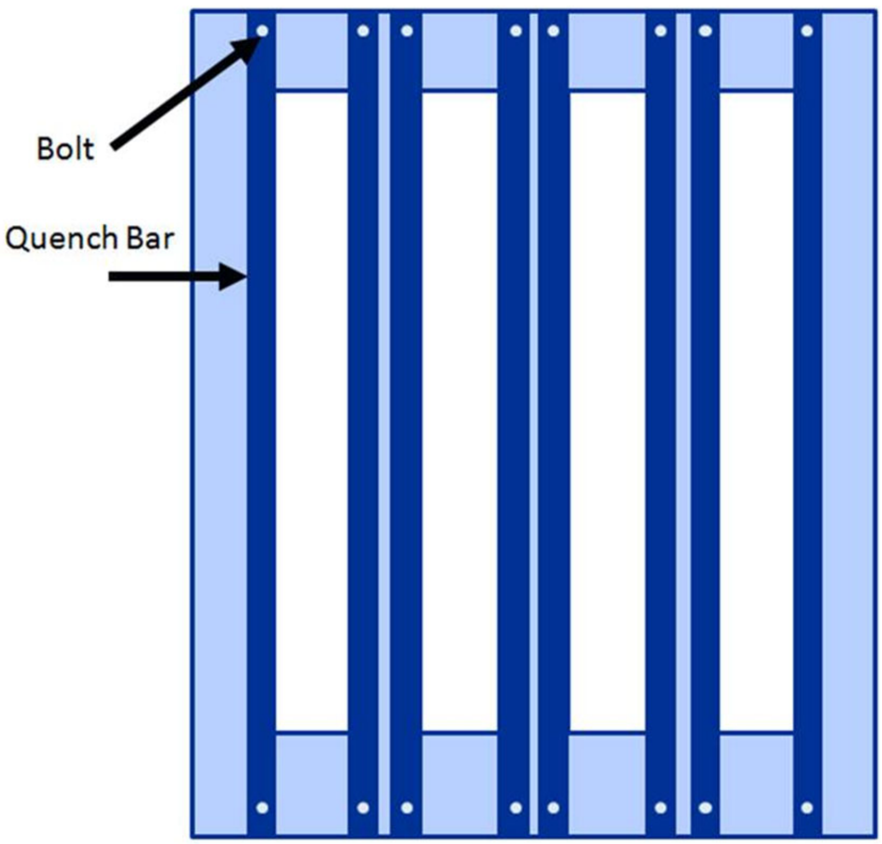

Figure 9.—Sample card with quench bars.

3.2 Data Acquisition, Storage and Archive

Data acquisition (DAQ) was achieved with an Agilent DAQ system supplied by the facility. The system supported two pressure transducers (one calibrated, one out of calibration), eight Type K thermocouples, two radiometers, two anemometers, and an igniter indication signal. Data was recorded at a rate of once per second. Plots of all test data were displayed on a computer monitor during testing. All raw test data was captured in Comma-Separated Values (CSV) format and read into a Microsoft Excel spreadsheet. Procedures for activating and using the DAQ are provided in Appendix J. Table 1 lists the experimental instrumentation and hardware used for data collection.

All Excel test data files, video files, and test matrices, are stored for archival on an external hard drive that was purchased by the task. Additionally, all of the Excel test data files and test matrices will be stored in the AES Spacecraft Fire Demonstration Project on eRoom. All Excel data files are labeled as VF13_"matrix name"_"mm/dd/yyyy"_"test/fill-run".xlsx, where matrix name is either DOE or SUP. For example, the filename for DOE test/fill 1, run 1 would be VF13_DOE_04052012_1-1.

4.0 Fuel Material

The leading fuel material candidates for the Large Scale Flight Experiment include cheesecloth and Solid Inflammability Boundary at Low-Speeds (SIBAL) material. The DOE did not include fuel as a variable parameter and therefore cheesecloth was the only fuel utilized for the DOE testing. Supplementary tests included SIBAL fuel. Details of each test and materials burned are provided in the test matrices included in Appendix C.

4.1 Cheesecloth

Cheesecloth is a loose-woven gauze-like cotton cloth available in many different grades/weaves. Four types of cheesecloth were ordered for this task; #50 unbleached, #60 unbleached, #90 unbleached, and #90 bleached. All were from www.cheesecloth.us. It was decided that #90 bleached would be the most appropriate cheesecloth selection for this test given its higher grade (more tightly woven fibers) lending itself to falling within a targeted area density. Additionally, samples of each type of cheesecloth were burn tested in a much smaller chamber. It was found that bleached cheesecloth burns more cleanly than unbleached which was more desirable for this test.

4.2 SIBAL

SIBAL fuel is a custom made cotton-fiberglass blend. When burning, the cotton is consumed leaving behind a fiberglass matrix after the flame passage. This material is capable of one-sided burning and may exhibit inconsistent flame spread rates. Only one roll was manufactured almost a decade ago and what remains of the roll is all that exists of the material today. The material was supplied by the GRC Combustion and Reacting Systems Branch, code REC. SIBAL is significantly less permeable than cheesecloth. It also proved to be easier to handle than cheesecloth in terms of sample preparation. The fabric was less prone to snagging, fraying and stretching.

5.0 Design of Experiments

The final DOE (JMP version 10.0) was an augmented custom design (build 1.3.2.20120426) consisting of five multi-level factors and one response as described in Table 2.

The selected response model contained main-effects with 2nd order interactions and included a constraint that disallowed non-physical combinations of the factors. The JMP software identified 28 runs necessary for an optimal design. Experiments were conducted utilizing the 4-slot sample holder such that two runs were performed for each VF-13 chamber test/fill. As such, 48 runs were identified and used in the DOE analysis. These runs included retests of anomalies and single point replicates. The relationship between the DOE name and name used for the response model is shown in Table 3.

TABLE 2.—DOE CUSTOM DESIGN

Component	DOE name	Levels
Continuous response	Delta P	Minimize
Categorical factors	Ignition location	B, T
-----------------------------	Quench block	N, Y
-----------------------------	Heat exchanger	N, L1, L2
Discrete numeric factors	FES width	12.5, 37.5 (cm)
-----------------------------	FES area	0.125, 0.375 (m^2)

TABLE 3.—DOE NAME VS. RESPONSE MODEL NAME

DOE name and relationship	Response model name
Delta P	Y
Ignition location	A
Quench block	B
Heat exchanger	C
(FES width-25)/12.5	X
(FES area-0.25)/0.125	Z

The response model expression is shown in Equation (1),

$$Y = \beta_0 + \beta_1 A + \beta_2 B + \beta_3 C + \beta_4 X + \beta_5 Z + \beta_6 AB + \beta_7 AC + \beta_8 AX + \beta_9 AZ + \beta_{10} BC + B_{11} BX + \beta_{12} BZ + \beta_{13} CX + \beta_{14} CZ \quad (1)$$

where the parameter estimates, β_j, are multi-valued for the categorical factors. Using a Standard Least Squares fit (normal assumptions apply), estimates for the response model parameters were determined and are shown in Table 4.

An Analysis of Variance provides a comparison between the fitted response model and a simple mean model. For this case, the results show (p-value <0.0001) that there is at least one significant effect in the response model with an R-squared value of 0.97 (estimates the proportion of variation in the response that can be attributed to the model rather than to random error). A graph of actual-versus-predicted Delta P is shown in Figure 10. The plot identifies the data points (markers), response model fit (solid red line) and 95 percent confidence interval (dashed red lines), and mean Delta P (dashed blue line). The final design (DOE test matrix), along with the experimental results for Delta P (calculated and verified) and the response model predicted Delta P can be found in Appendix C and Appendix K, respectively.

TABLE 4.—RESPONSE MODEL ESTIMATES

Parameter	Factor	Factor level	Estimate
β_0	Intercept	Intercept	0.370
β_1	A	B	0.186
--	--	T	–0.186
β_2	B	N	0.045
--	--	Y	–0.045
β_3	C	N	0.130
--	--	L1	0.062
--	--	L2	–0.192
β_4	X	--	0.076
β_5	Z	--	0.109
β_6	AB	B, N	0.030
--	--	B, Y	–0.030
--	--	T, N	–0.030
--	--	T, Y	0.030
β_7	AC	B, N	0.119
--	--	B, L1	0.038
--	--	B, L2	–0.158
--	--	T, N	–0.119
--	--	T, L1	–0.038
--	--	T, L2	0.158
β_8	AX	B	0.027
--	--	T	–0.027
β_9	AZ	B	0.096
--	--	T	–0.096
β_{10}	BC	N, N	0.005
--	--	N, L1	–0.010
--	--	N, L2	0.006
--	--	Y, N	–0.005
--	--	Y, L1	0.010
--	--	Y, L2	–0.006
β_{11}	BX	N	0.034
--	--	Y	–0.034
β_{12}	BZ	N	0.004
--	--	Y	–0.004
β_{13}	CX	N	0.016
--	--	L1	–0.005
--	--	L2	–0.011
β_{14}	CZ	N	0.046
--	--	L1	0.035
--	--	L2	–0.081

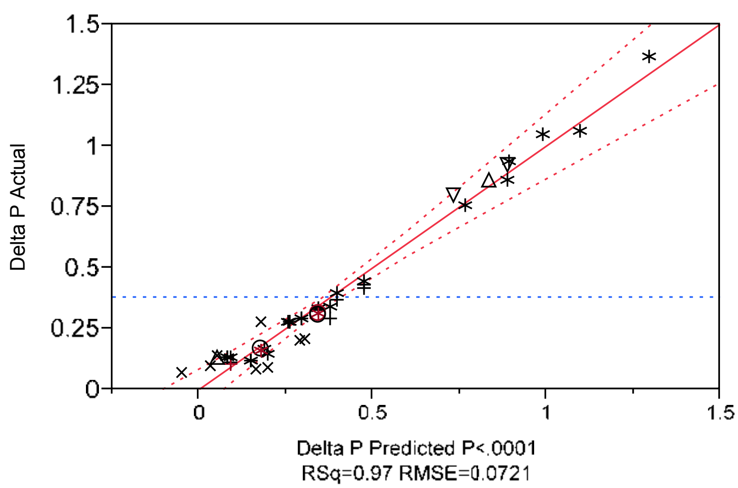

Figure 10.—Actual vs. Predicted Delta P.

6.0 Results

The volume of data collected from the experiment was substantial. Each archived data file includes plots of the pressure transducer, thermocouple, anemometer, and radiometer readings. In lieu of capturing every data plot from each test within this report, the following sections highlight only select test data. Future publications will address and evaluate empirical relationships, trends, and correlations.

6.1 Pressure Plot Examples and Pressure Trends

Given the main test objective, the majority of the selected example plots to follow are pressure data plots. One pressure plot was selected to illustrate each test parameter. Trends in the pressure data were captured in a series of plots meant to group pressure outcomes according to categorical parameters. These are also included within the following subsections. The change in pressure for each test in both the DOE and Supplementary test sets is included in Appendix L. Several still pictures captured from the video files highlighting depictions of various test parameters are in Appendix M.

6.1.1 Top vs. Bottom Ignition

The following plots in Figures 11 and 12, show the difference in pressure rise between the two ignition locations investigated during these tests. The plots shown below are for similar cases; a single 12.5 cm wide sample without quench bars and without a heat exchanger. Ignition at the top of a sample yields a much slower burn time and less intense flame than a bottom ignition. As a result, the peak pressure for a top ignition will not be as high as the peak pressure for a bottom ignition for otherwise equivalent cases. Additionally, the peak pressure takes longer to reach as a result of a longer duration burn with a top ignition.

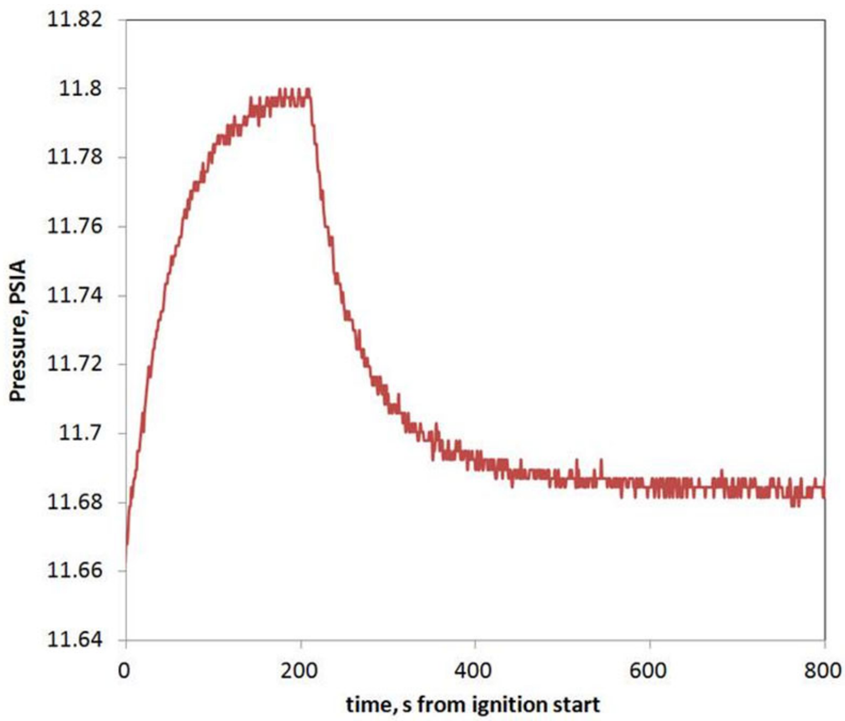

Figure 11.—DOE test 1-1 top ignition example pressure plot.

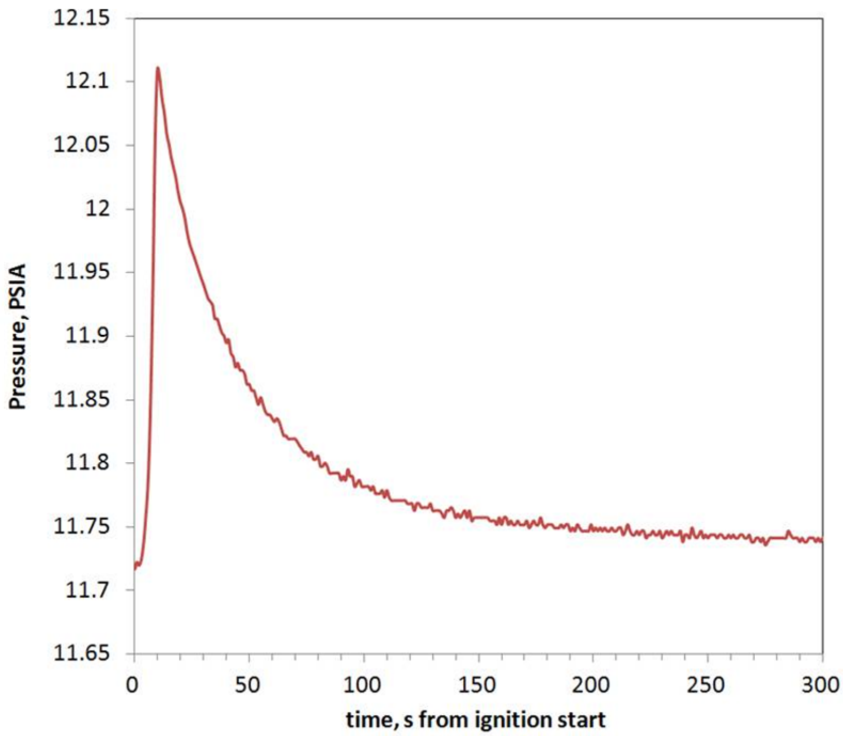

Figure 12.—DOE test 3-6 bottom ignition example pressure plot.

6.1.2 Simultaneous vs. Sequential Sample Ignition

The following plots in Figures 13 to 16, show the difference in pressure rise between igniting multiple samples simultaneously and sequentially (also referred to as "in series"). The plots shown below are for similar cases. The first two plots are for cases burning three 12.5 cm wide samples ignited at the bottom without quench bars and without a heat exchanger. The second two cases are for burning three 12.5 cm wide samples ignited at the top without quench bars and without a heat exchanger. While total pressure rise appears to be different between the bottom ignition cases it is very close to the same. The apparent difference is caused by lag time while igniting sequentially as a result of test operator inaccuracies. The total pressure rise between the top ignition cases is slightly different. The sample material takes much longer to burn downward with a top ignition than upward with a bottom ignition, therefore sequential burns compared to simultaneous burns of the same amount of material at the same conditions will likely yield a lower total pressure rise. This is due in part to the released heat having more time to be absorbed by the surroundings.

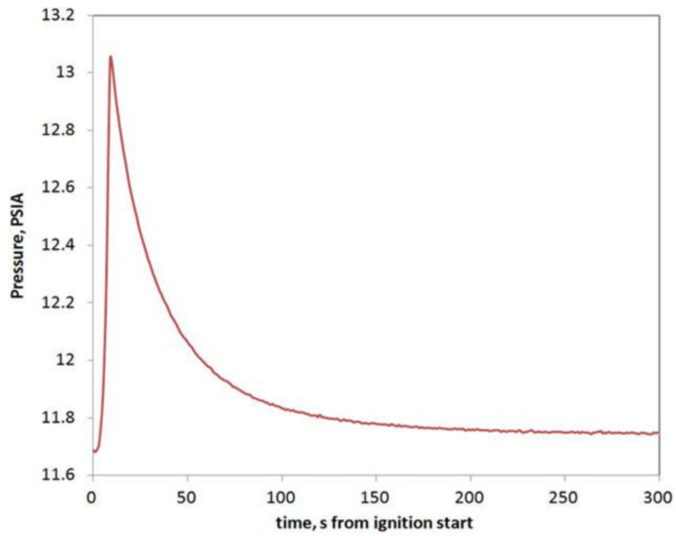

Figure 13.—DOE test 1-2 simultaneous bottom ignition example pressure plot.

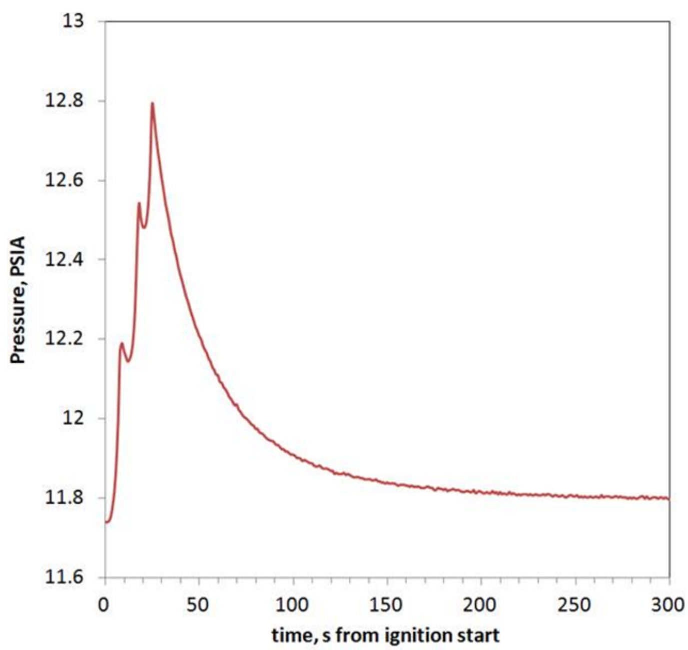

Figure 14.—DOE test 2-4 sequential bottom ignition example pressure plot.

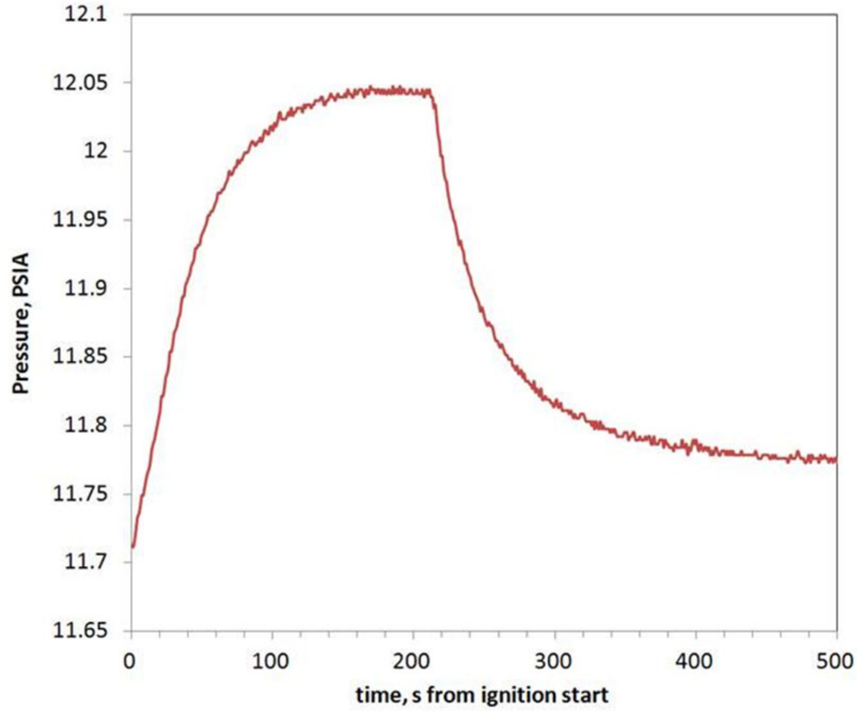

Figure 15.—DOE test 7-14 simultaneous top ignition example pressure plot.

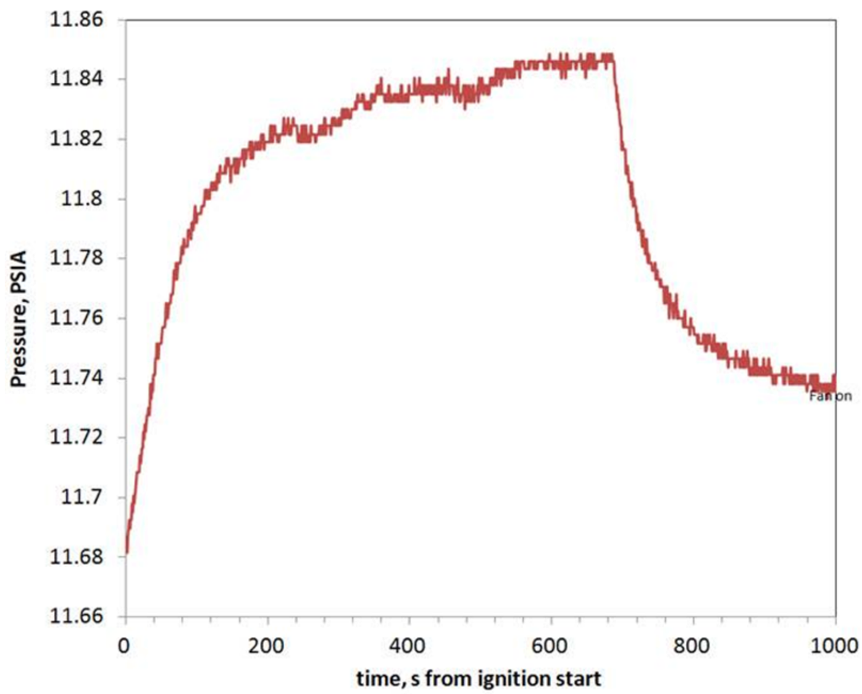

Figure 16.—DOE test 20-39 sequential top ignition example pressure plot.

6.1.3 Quench Bars: With vs. Without

The following plots in Figures 17 and 18, show pressure rise for cases with quench bars and without. The plots shown are for similar cases; three samples simultaneously ignited at the top without a heat exchanger. The plots are so similar that it is difficult to visually see any obvious differences in pressure patterns. Any quench bar influences are more easily seen in later plots in section 6.1.6.

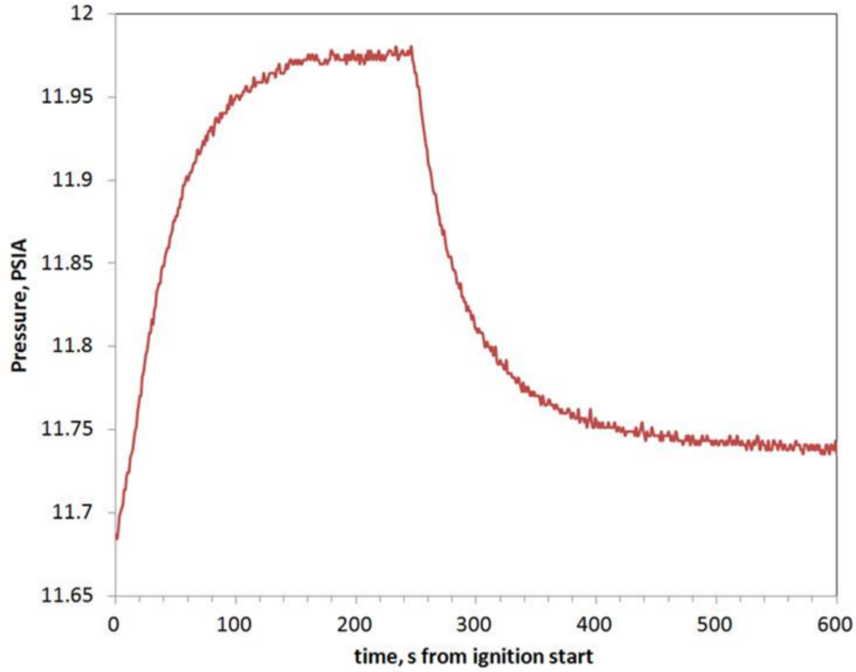

Figure 17.—DOE test 22-43 no quench bars example pressure plot.

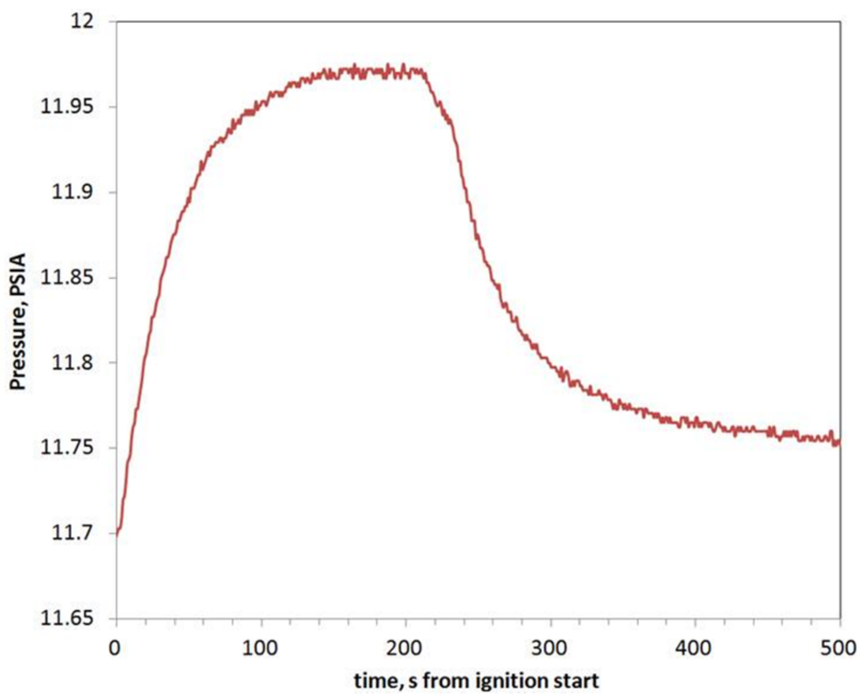

Figure 18.—DOE test 23-45 with quench bars example pressure plot.

6.1.4 Heat Exchanger: With vs. Without

The following plots in Figures 19 to 21, show pressure rise for cases with each of the two heat exchangers and without. The plots shown are for similar cases; a single 12.5 cm wide sample ignited at the bottom without quench bars. As with the quench bars, the pressure plots for the case without the heat exchanger and the case with the L1 heat exchanger are so similar that it is difficult to observe the difference, if any, in the total pressure rise. The effect of the L1 heat exchanger is more easily seen in later plots in the Pressure Trends section. It is evident that the total pressure rise in the L2 heat exchanger case was lower than the case without a heat exchanger.

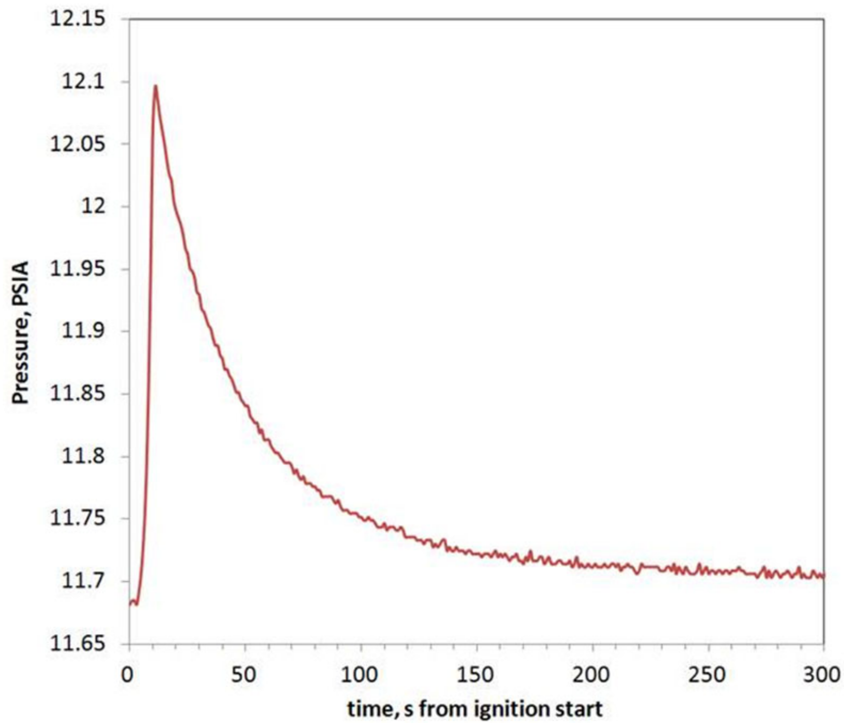

Figure 19.—DOE test 10-19 no heat exchanger example pressure plot.

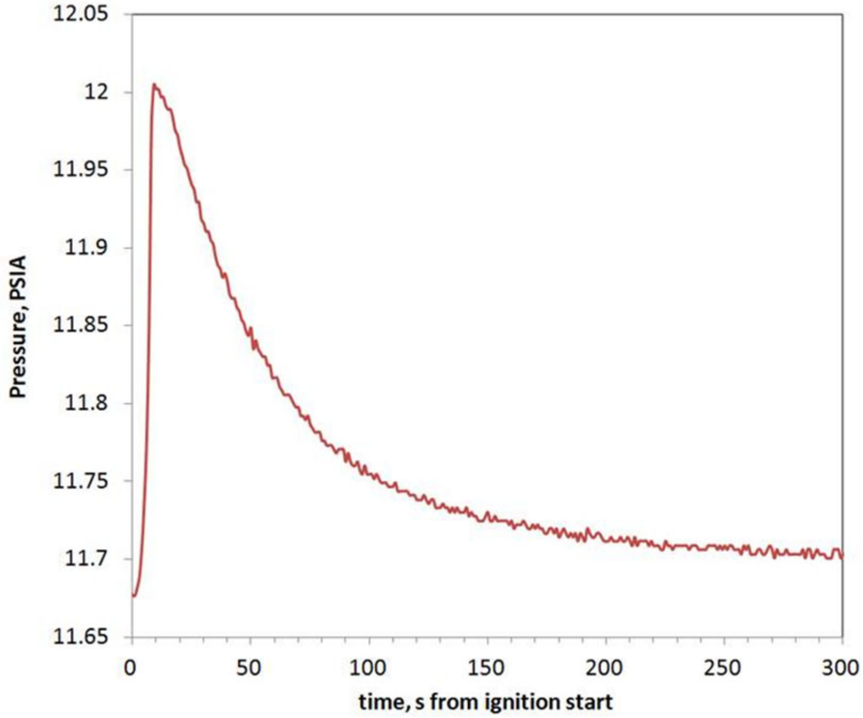

Figure 20.—DOE test 14-27 L1 heat exchanger example pressure plot.

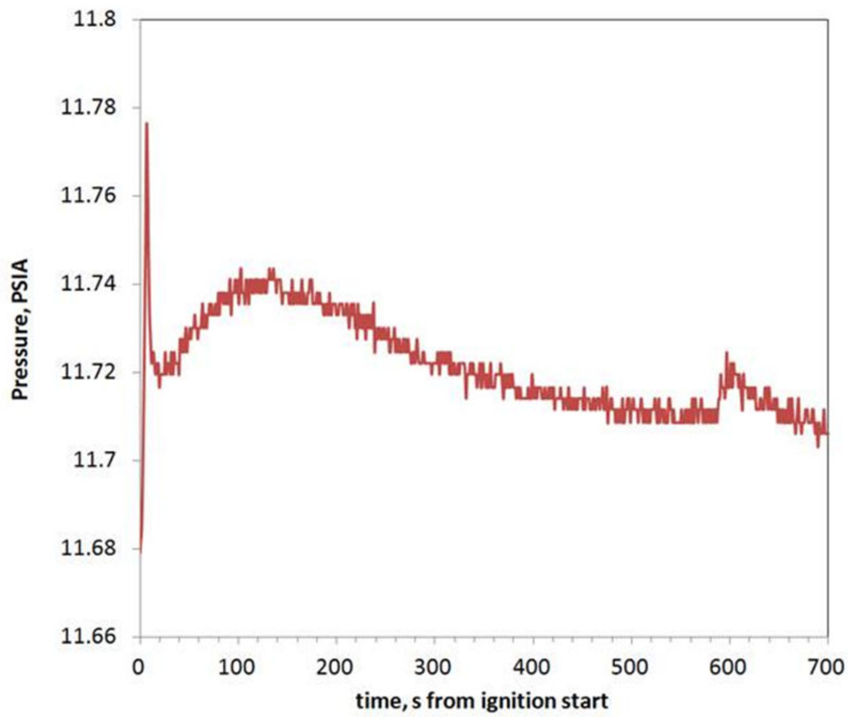

Figure 21.—DOE test 17-33 L2 heat exchanger example pressure plot.

6.1.5 Cheesecloth vs. SIBAL

The following plots in Figures 22 and 23, show the difference in pressure rise between burning cheesecloth and SIBAL material. The plots shown are for similar cases; one 50 cm wide by 100 cm long sample ignited at the bottom without quench bars and without a heat exchanger. Burning SIBAL fuel yields a greater pressure rise than burning the same size sample of cheesecloth (despite the starting pressure being lower in this particular SIBAL test case). This is to be expected since the area density of SIBAL is greater than cheesecloth. SIBAL fuel burns more slowly than cheesecloth and consequently its pressure rise curve is more symmetric than the curve for cheesecloth.

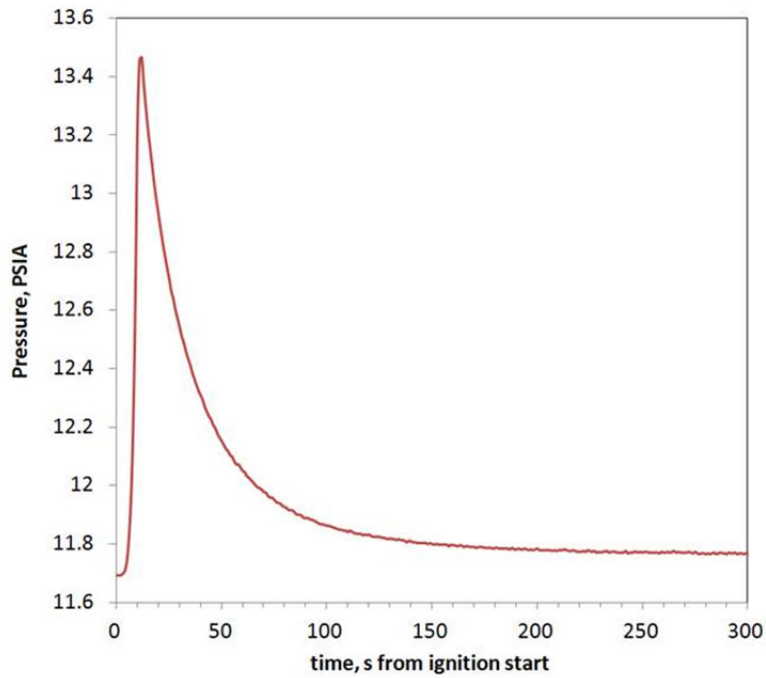

Figure 22.—SUP test 4-5 50×100 cm cheesecloth example pressure plot.

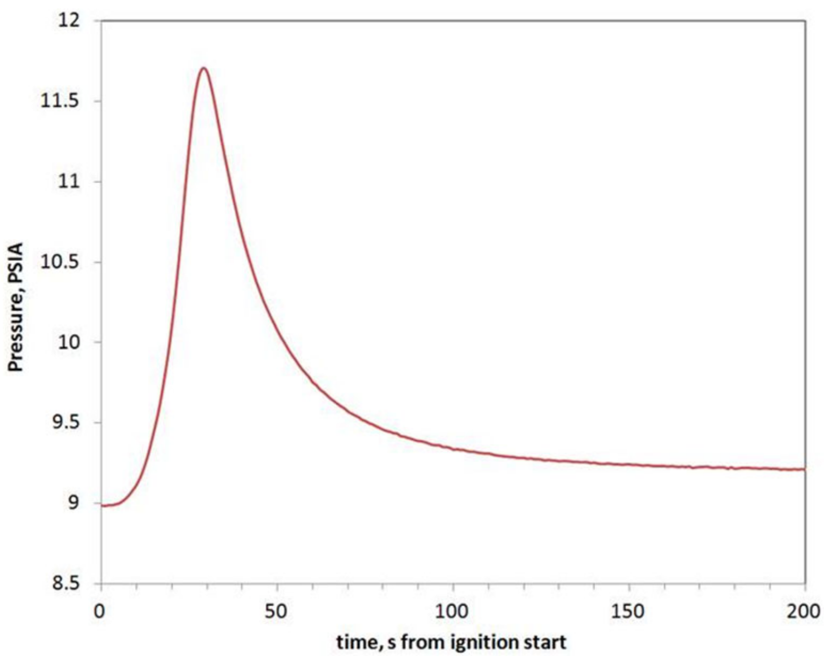

Figure 23.—SUP test 14-21 50×100 cm SIBAL example pressure plot.

6.1.6 Pressure Trends

To facilitate evaluating data from the tests, pressure trends from the DOE test runs are combined in the following plots in Figures 24 to 30. The data is separated categorically for visualization. References to top ignition or bottom ignition are synonymous with downward and upward burning, respectfully.

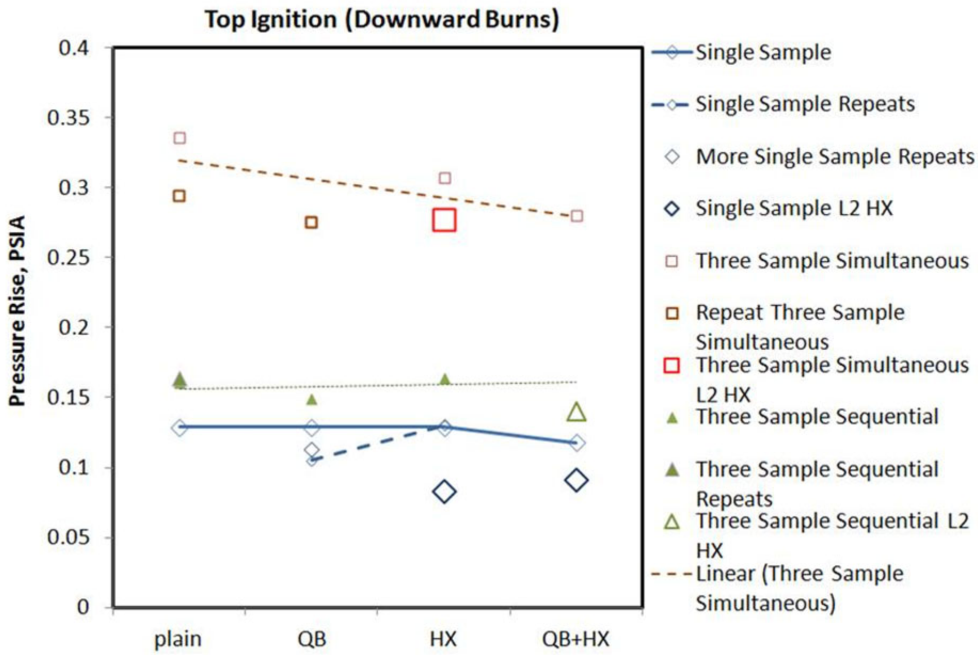

Figure 24.—Top ignition DOE test runs by categorical parameter.

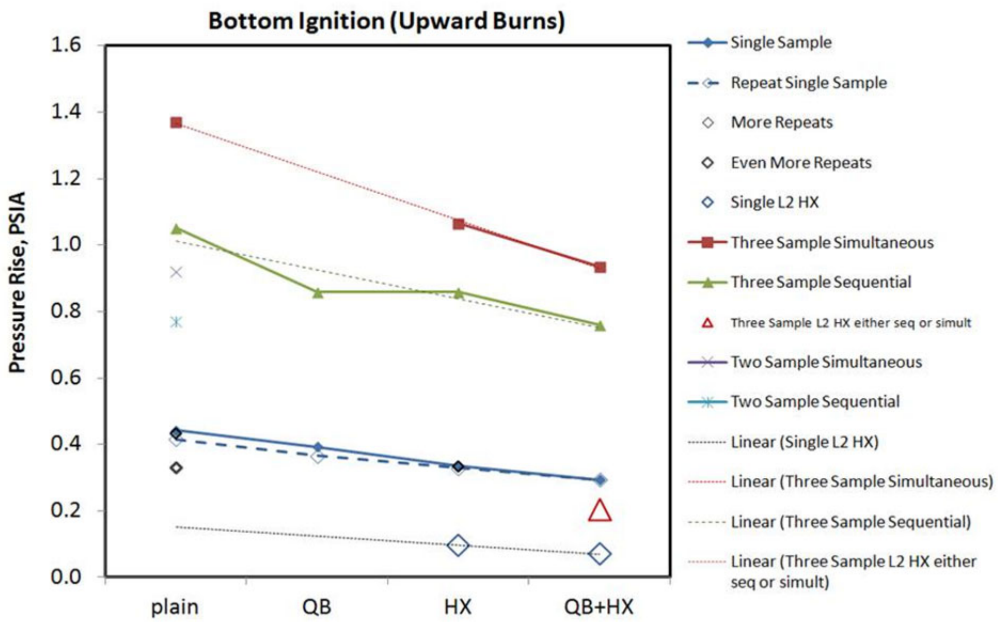

Figure 25.—Bottom ignition DOE test runs by categorical parameter.

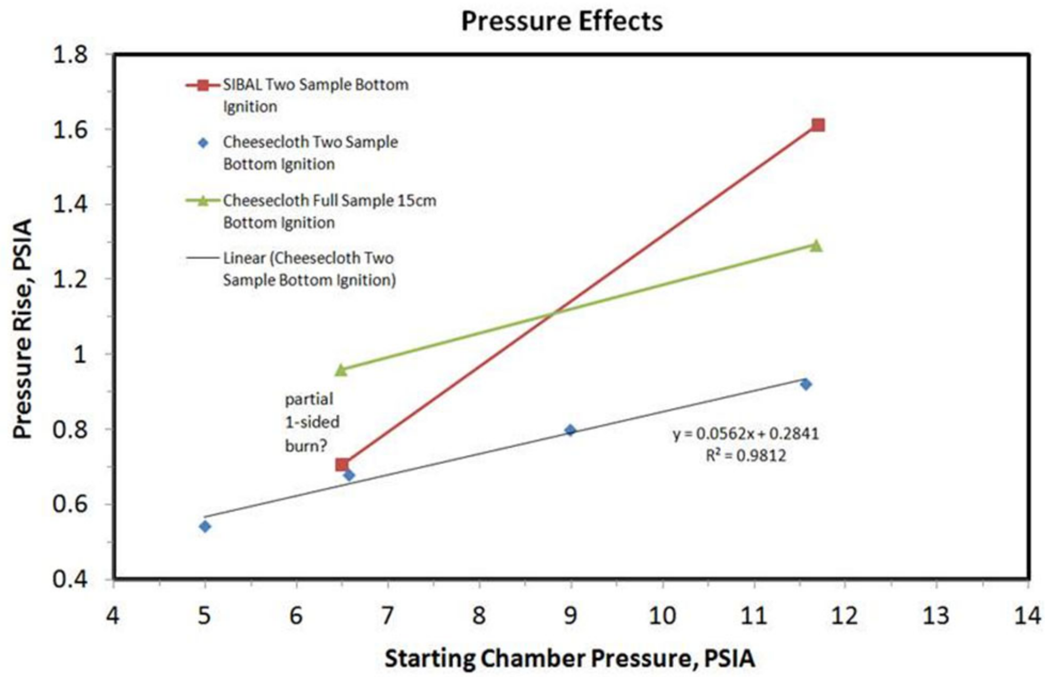

Figure 26.—Effect of starting chamber pressure.

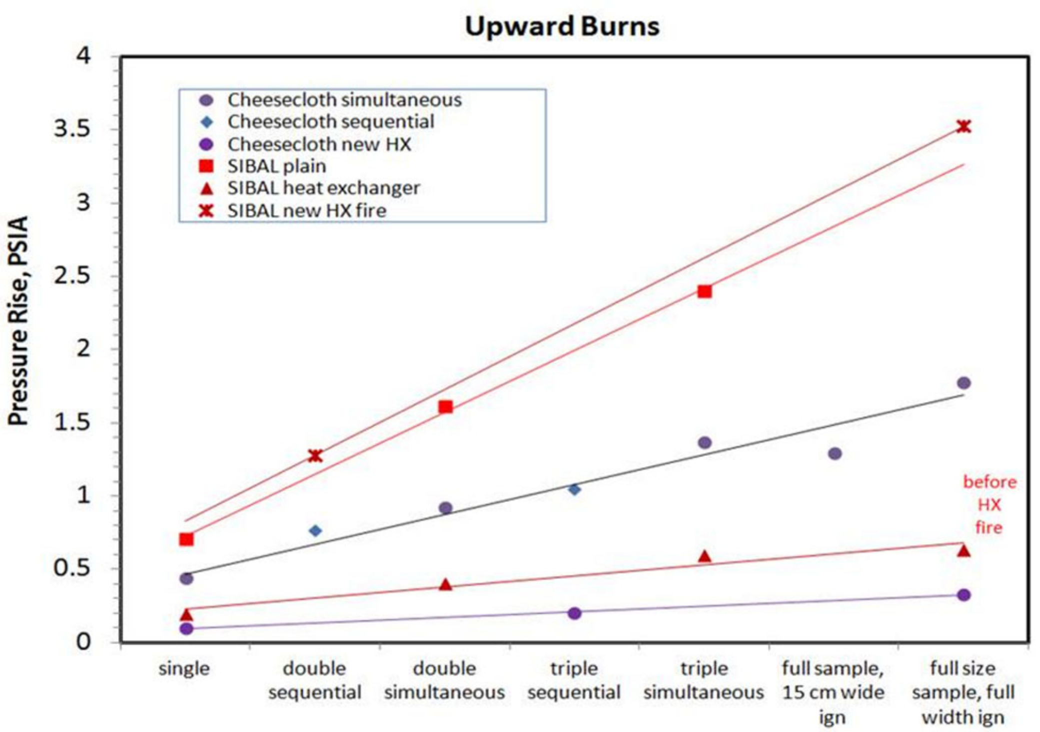

Figure 27.—Top ignition pressure rise by number of samples (sheets).

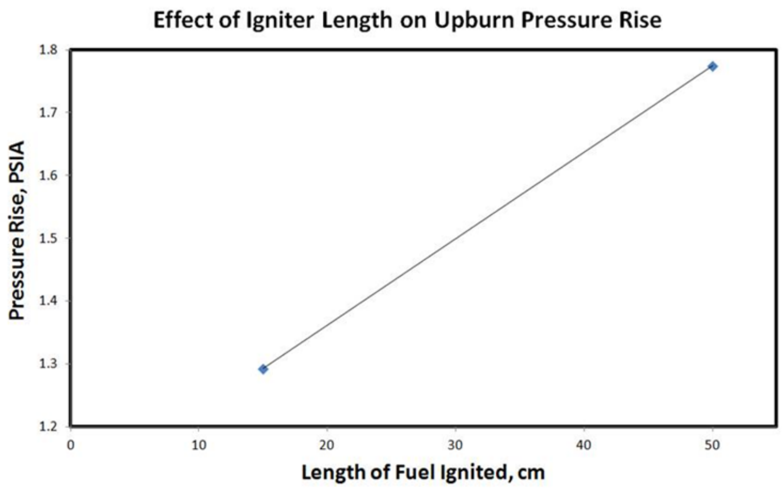

Figure 28.—Igniter length effects on bottom ignition pressure rise.

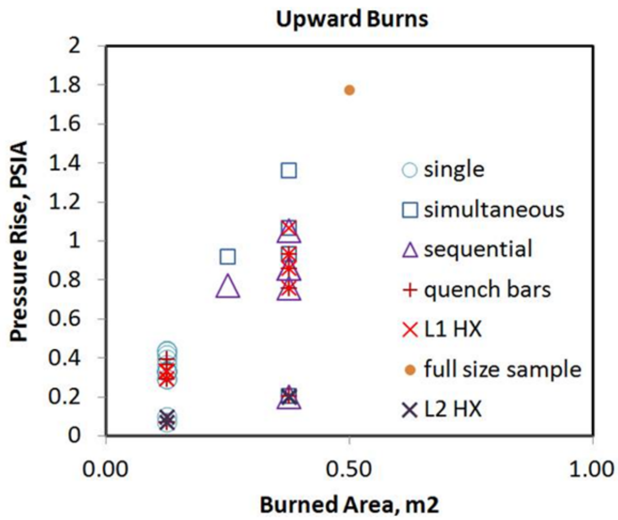

Figure 29.—Pressure rise versus area burned for upward burns.

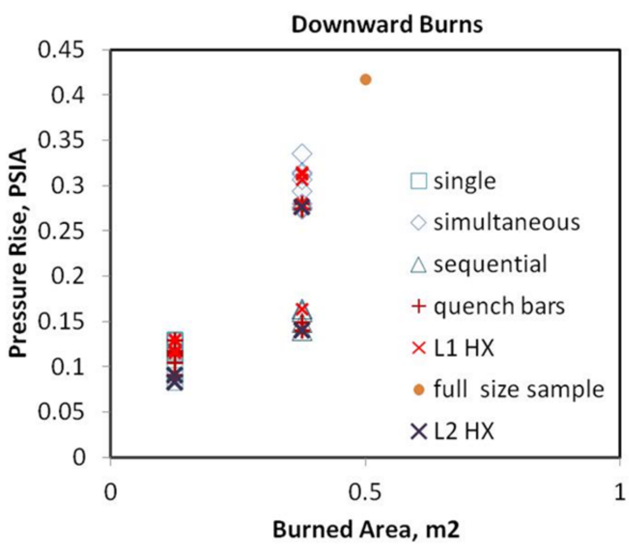

Figure 30.—Pressure rise versus area burned for downward burns.

6.2 Temperature Data Plot

The following plot in Figure 31 shows the temperature response for three samples of cheesecloth ignited from the top and burned sequentially with quench bars. As each sample was burning, the thermocouple(s) directly above it were the most reactive and had the largest swing in temperature response.

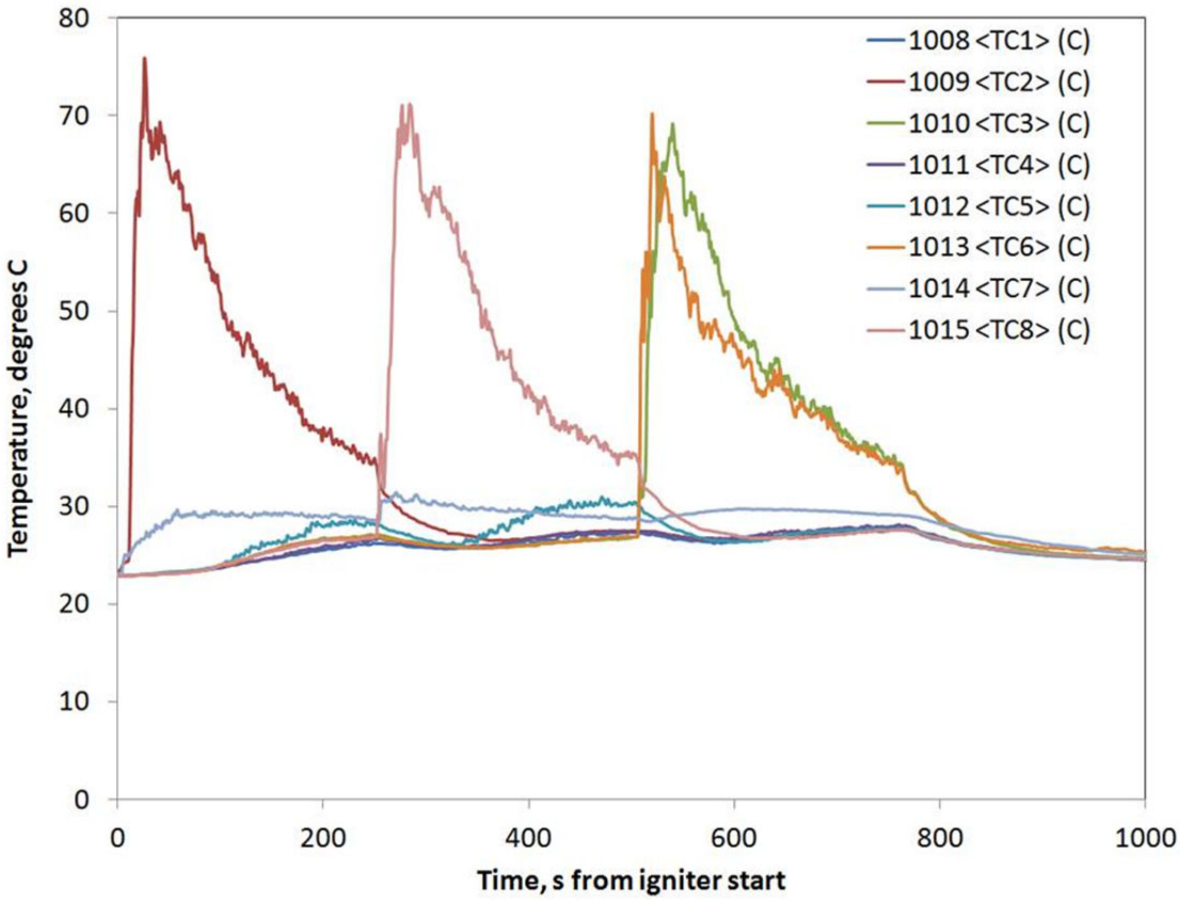

Figure 31.—DOE test 10-20 temperature data plot.

6.3 Anemometer Data Plot

The following plot in Figure 32 shows the airspeed response for three samples of cheesecloth ignited from the top and burned simultaneously. There are two obvious periods of air disturbance during the test. The first is in response to the cheesecloth burning and creating buoyant flow. The second occurs while the mixing fan is operational. It can be seen that the anemometers saturate at a reading of approximately 55 cm/s which is reached by one of them during fan mixing. It can also be seen that the anemometer readings are not congruent. In addition to the placement of the anemometers with respect to the samples, the asymmetry of the interior bottom section of the test chamber likely contributed to this.

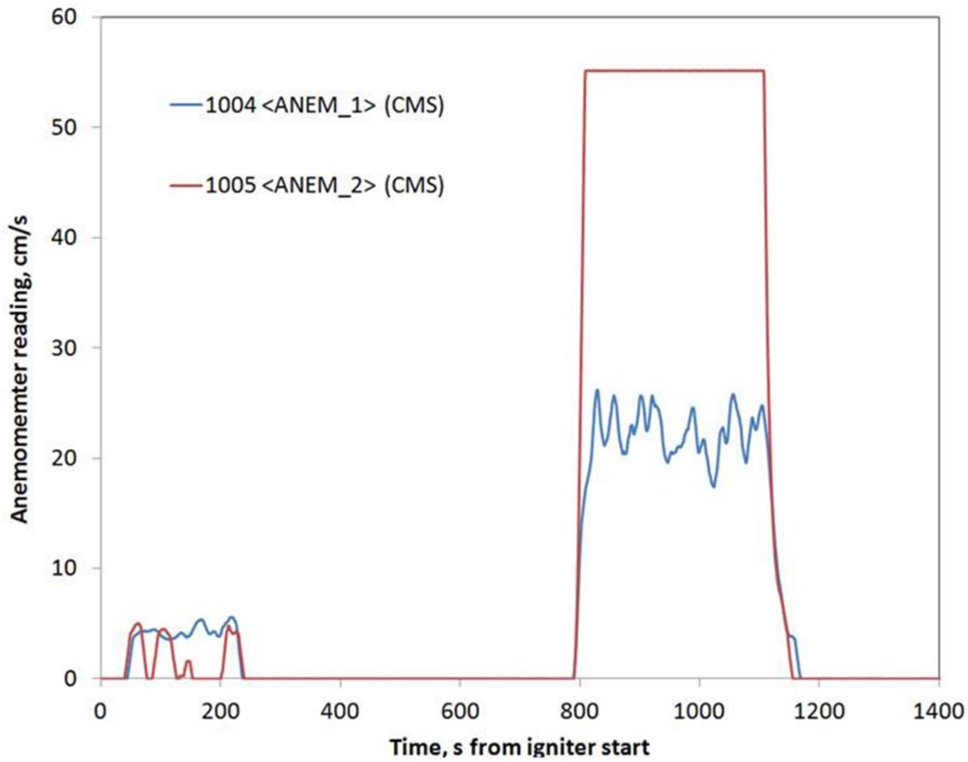

Figure 32.—DOE test 7-14 anemometer data plot.

6.4 Radiometer Data Plot

The following plot in Figure 33 shows the radiometer readings for three samples of cheesecloth ignited from the top and burned simultaneously. The radiometer signals were output as a voltage rather than converted directly into a reading of radiant flux. The radiometer readings were suitable for indicating an accurate estimate of total burn time. While not shown in this plot, the radiometers saturate at approximately 8.5 V.

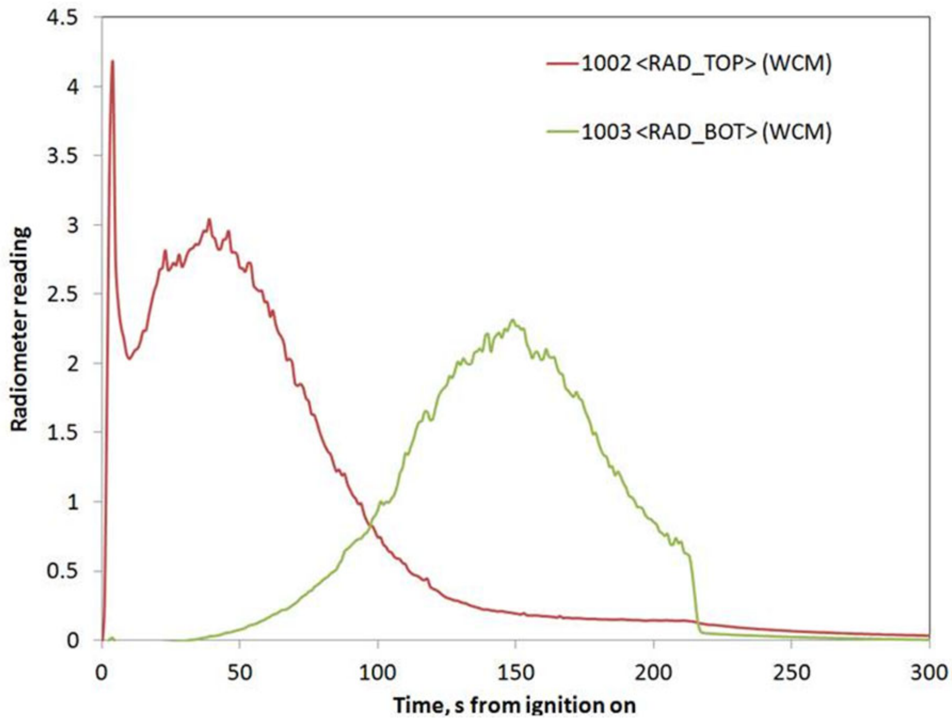

Figure 33.—DOE test 7-14 radiometer data plot.

6.5 Determining Burn-Times From Radiometer Data

A quantitative approach based on radiometer data was developed in order to avoid subjectivity to determine burn-times from the VF-13 tests. The analysis includes single-, double-, and triple-strip samples and full-size samples where the multiple samples are ignited simultaneously and the full-size samples are ignited along their full width. Repeat tests are also included, but multiple samples with serial ignitions (i.e., sequential burns) are ignored in the analysis. The anomalous tests are excluded. For DOE run 2.3, the radiometers seem dysfunctional, therefore this test is also excluded.

For the downward burn cases where the samples are ignited at the top, the "ignition time" is obtained from the time corresponding to the first 30 percent reading of the full range of the top radiometer (while taking off), and the "extinction time" is obtained from the time corresponding to the second 30 percent reading of the full range of the bottom radiometer (while falling down). The term "full range" is defined as the difference between the maximum and minimum values of the radiometer reading. The burn-times are obtained from the difference of extinction and ignition times. Error bars indicate one standard deviation of all relevant data including repeats. No error bar means that there is only one single run of that given case.

For the upward burn cases where the samples are ignited from the bottom, all of the radiometer readings saturate except the single-strip burns. Therefore, the radiative heat loss evaluation of double-strip, triple-strip, and full-size sample tests are not possible. Also, the radiometer readings for many tests do not come down to their original minimum after the burns and seem to settle at a higher value (just like the pressure curves). Under the circumstances, the approach adopted to determine the extinction time for downburn cases is modified in order to handle the upburn cases in a more rational and consistent way. The determination of the ignition times for the upburn cases are kept the same as the downburn cases since the radiometer behavior is unaffected during ignitions of either cases. For determining the extinction times of upburn cases, 50 percent full-scale readings give reasonable values for these fast burns which last only about 9 sec (where "full scale" means the saturation value). Since the data is recorded every second, obtaining burn-times require some interpolations of readings at two consecutive seconds.

The data presented are for either cheesecloth or SIBAL fuel material. The cheesecloth data includes all DOE tests and some of the relevant Supplemental tests while the SIBAL data is taken only from Supplemental tests. All tests had an initial pressure of about 11.7 psi (~0.8 atm) except where indicated otherwise. The pressure effect data is obtained from single tests of double-strip cheesecloth samples.

6.5.1 Cheesecloth Burn-Times

Tables 5 and 6 and Figures 34 to 36, give the upward burn cases first followed by the downward burn cases. Burn-times labeled as "measured" are obtained from radiometer data as described above.

TABLE 5.—CHEESECLOTH BURN-TIMES FOR UPWARD BURNING (BOTTOM IGNITION)

(yellow)	sequential burn; not considered for burn-times
(red)	anomalous tests; not considered
(magenta)	radiometer dysfunctional

All tests had an initial pressure of about 11.7 psi (~ 0.8 atm) except where indicated in aqua color.

Ignition location	Quench block (QB)	Heat exchanger (HX)	Sample width (cm)	Sample area (cm^2)	Measured deltaP (psi)	Burn-time (s)	Run.Fill numbers, test dates & comments
B	N	N	12.5	0.125	0.442	7.44	7.13 (4/24/12)
B	N	N	12.5	0.125	0.415	8.64	10.19 (5/2/12); replicate of 7.13
B	N	N	12.5	0.125	0.434	7.92	22.44 (6/1/12); replicate of 7.13
B	N	N	12.5	0.125	0.431	7.58	23.46 (6/4/12); replicate of 7.13
B	N	N	25.0	0.250	0.921	9.92	Supp1.1 (3/29/12); check out
B	N	N	37.5	0.375	1.369	8.93	1.2 (4/5/12)
B	N	N	50.0	0.500	1.776	9.82	Supp4.5 (5/3/12); full sample
B	N	N	12.5	0.375	1.051		2.4 (4/10/12); sequential burn
B	N	N	12.5	0.250	0.797		CO.b (3/29/12); check out; sequential burn
B	Y	N	12.5	0.125	0.394	8.16	3.6 (4/16/12)
B	Y	N	12.5	0.125	0.366	7.56	11.21 (5/3/12); replicate of 3.6
B	Y	N	12.5	0.375	0.859		12.24 (5/4/12); sequential burn
B	N	Y/HX1	12.5	0.125	0.334	7.06	6.11 (4/20/12)
B	N	Y/HX1	12.5	0.125	0.329	7.29	14.27 (5/9/12); replicate of 6.11
B	N	Y/HX1	12.5	0.125	0.334	7.64	21.42 (5/31/12); replicate of 6.11
B	N	Y/HX1	37.5	0.375	1.065	9.40	8.16 (4/26/12)
B	N	Y/HX1	12.5	0.375	0.860		5.10 (4/19/12); sequential burn
B	N	Y/HX2	12.5	0.125	0.097	7.80	17.33 (5/24/12)
B	N	Y/HX2	50.0	0.500	0.326	9.97	Supp11.17 (6/6/12); full sample
B	N	Y/HX2	12.5	0.375	0.202		16.32 (5/23/12); sequential burn
B	Y	Y/HX1	12.5	0.125	0.294	7.46	9.17 (4/30/12)
B	Y	Y/HX1	12.5	0.125	0.294	7.62	13.25 (5/7/12); replicate of 9.17
B	Y	Y/HX1	37.5	0.375	0.935	9.60	4.8 (4/17/12)
B	Y	Y/HX1	12.5	0.375	0.759		14.28 (5/9/12); sequential burn
B	Y	Y/HX2	12.5	0.125	0.070	7.70	18.35 (5/25/12)
B	Y	Y/HX2	37.5	0.375	0.205	9.93	18.36 (5/25/12)
B	N	N	12.5	0.250	0.800	10.18	Supp13.20 (6/8/12); initial P: 9 psi
B	N	N	12.5	0.250	0.679	13.56	Supp10.16 (5/22/12); initial P: 6.6 psi
B	N	N	12.5	0.250	0.541	18.40	Supp13.19 (6/8/12); initial P: 5 psi

TABLE 6.—CHEESECLOTH BURN-TIMES FOR DOWNWARD BURNING (TOP IGNITION)

(yellow)	sequential burn; not considered for burn-times
(red)	anomalous tests; not considered
(magenta)	radiometer dysfunctional

All tests had an initial pressure of about 11.7 psi (~ 0.8 atm) except where indicated in aqua color.

Ignition location	Quench block (QB)	Heat exchanger (HX)	Sample width (cm)	Sample area (cm^2)	Measured deltaP (psi)	Burn-time (s)	Run.Fill numbers, test dates & comments
T	N	N	12.5	0.125	0.129	211.50	1.1 (4/5/12)
T	N	N	37.5	0.375	0.337	209.00	7.14 (4/24/12)
T	N	N	37.5	0.375	0.294	243.45	22.43 (6/1/12); replicate of 7.14
T	N	N	12.5	0.375	0.161		11.22 (5/3/12); sequential burn; anomaly
T	N	N	12.5	0.375	0.164		20.39 (5/30/12); retest of 11.22; sequential burn
T	Y	N	12.5	0.125	0.130		2.3 (4/10/12); radiometer dysfunctional
T	Y	N	12.5	0.125	0.105		12.23 (5/4/12); replicate of 2.3; anomaly
T	Y	N	12.5	0.125	0.113	240.75	20.40 (5/30/12); replicate of 2.3
T	Y	N	37.5	0.375	0.275	245.25	3.5 (4/16/12)
T	Y	N	37.5	0.375	0.275	212.00	23.45 (6/4/12); replicate of 3.5
T	Y	N	12.5	0.375	0.149		10.20 (5/2/12); sequential burn
T	N	Y/HX1	12.5	0.125	0.129	223.24	4.7 (4/17/12)
T	N	Y/HX1	12.5	0.125	0.130	222.77	5.9 (4/19/12), Replicate of 4.7
T	N	Y/HX1	37.5	0.375	0.315		9.18 (4/30/12); anomaly
T	N	Y/HX1	37.5	0.375	0.313		13.26 (5/7/12); retest of 9.18; anomaly
T	N	Y/HX1	37.5	0.375	0.307	224.54	21.41 (5/31/12); retest of 9.18
T	N	Y/HX1	12.5	0.375	0.164		15.30 (5/10/12); sequential burn
T	N	Y/HX2	12.5	0.125	0.084	243.25	16.31 (5/23/12)
T	N	Y/HX2	37.5	0.375	0.278	243.37	17.34 (5/24/12)
T	Y	Y/HX1	12.5	0.125	0.118	217.50	8.15 (4/26/12)
T	Y	Y/HX1	12.5	0.125	0.116	226.77	15.29 (5/10/12); replicate of 8.15
T	Y	Y/HX1	37.5	0.375	0.281	207.50	6.12 (4/20/12)
T	Y	Y/HX2	12.5	0.125	0.091	251.00	19.37 (5/29/12)
T	Y	Y/HX2	12.5	0.375	0.140		19.38 (5/29/12); sequential burn

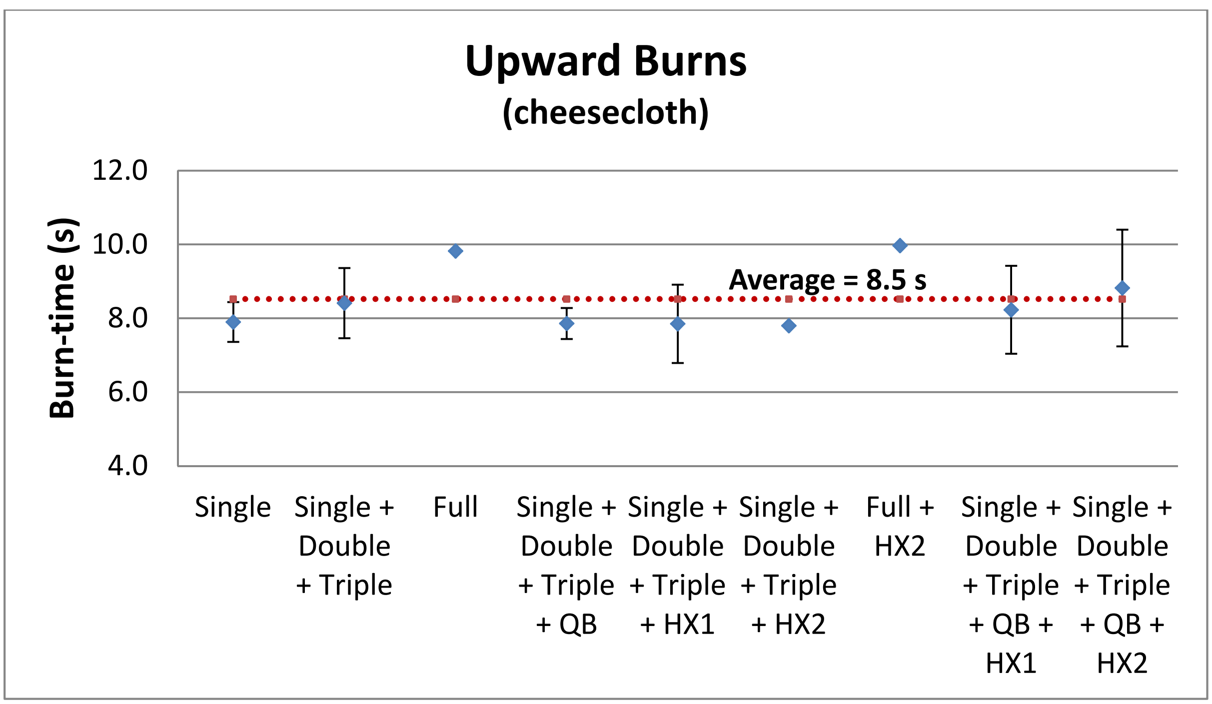

Figure 34.—Burn-times for cheesecloth upward burns.

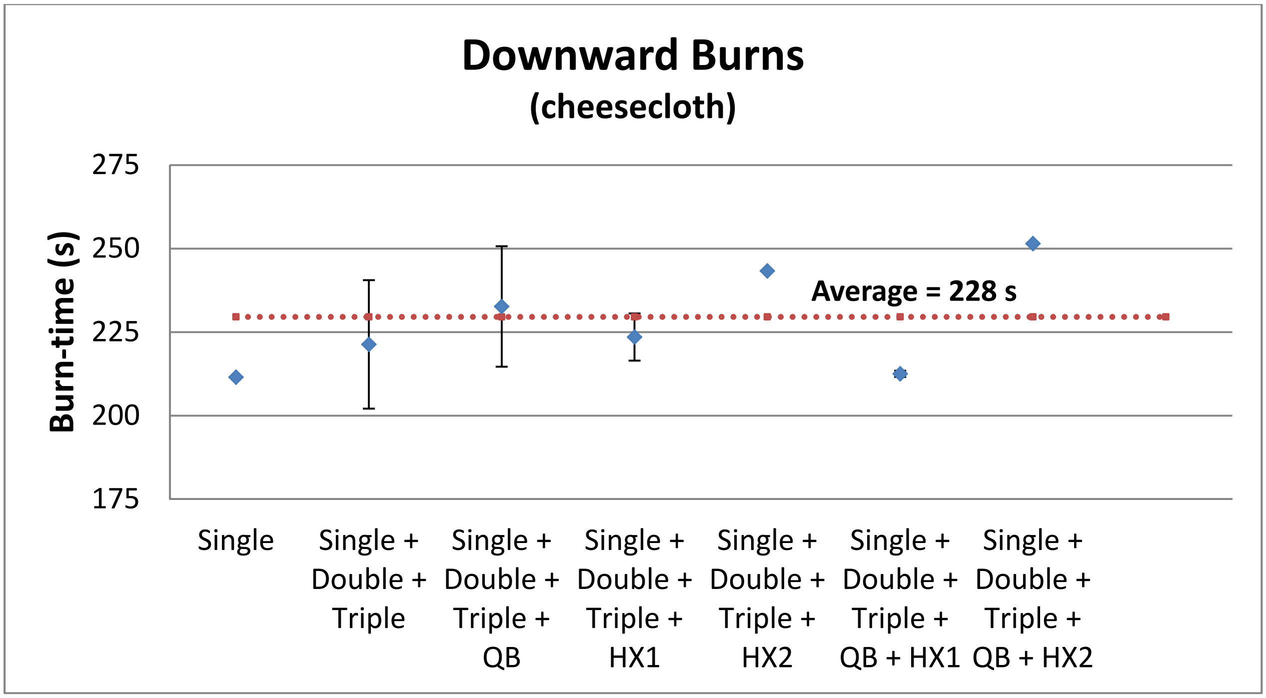

Figure 35.—Burn-times for cheesecloth downward burns.

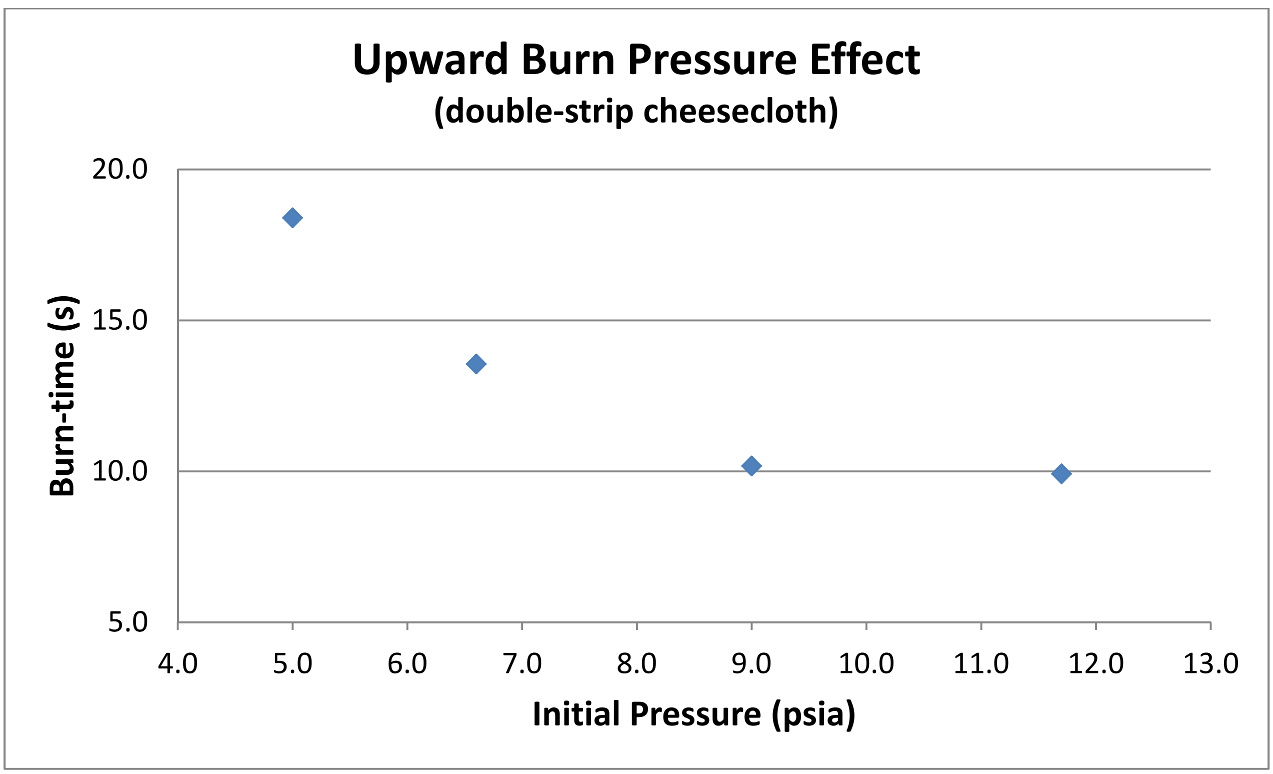

Figure 36.—Cheesecloth upward burn pressure effect.

6.5.2 SIBAL Cloth Burn-Times

SIBAL cloth is a composite fuel material with a total area density of 18.05±0.02 mg/cm^2 and thickness of 0.31±0.02 mm, composed of 75 percent cotton and 25 percent fiberglass by mass. Only the cotton portion is burned and the fiberglass skeleton structure remains after burns. In terms of relative energy densities, SIBAL cloth fuel releases about 3.2 times more heat per unit area than cheesecloth.

Even though the flame spread rates on SIBAL cloth are slower than those on cheesecloth, due to the larger area density of SIBAL cloth (18.05 vs. 4.28 mg/cm^2), the more energetic burns of SIBAL fuel lead to greater radiation. This results in faster saturation of the radiometers beyond their applicable scale and longer periods of recovery for the radiometer readings to fall back to their measurement range. Furthermore, after each burn, it has experimentally been observed that the remaining skeleton of SIBAL cloth fuel continues to glow partially due to the continued smoldering of cotton stuck on fiberglass structure and partially due to decaying radiation from warm fiberglass after the flame passes while it is cooling. SIBAL burning data is shown in Table 7 and Figures 37 and 38.

These factors render the approach to use radiometer readings to determine burn-times impractical for SIBAL fuel. Although the determination of ignition times may be acceptable, the determination of extinction times for SIBAL cloth burns is highly unreliable, as reflected in the table and graph below. For the nominal initial pressure cases when no heat exchanger is used, the burn-times of various-width samples are expected to be close to one another. Yet, they are considerably different. Therefore, it is recommended that some method other than using radiometer readings be adopted to determine the burn-times of SIBAL cloth cases.

TABLE 7.—SIBAL CLOTH BURN-TIMES FOR UPWARD BURNING (BOTTOM IGNITION)

(yellow)	sequential burn; not considered for burn-times
(red)	anomalous tests; not considered
(magenta)	radiometer dysfunctional

All tests had an initial pressure of about 11.7 psi (~ 0.8 atm) except where indicated in aqua color.

Fuel: SIBAL cloth

Ignition location	Quench block (QB)	Heat exchanger (HX)	Sample width (cm)	Sample area (cm^2)	Measured deltaP (psi)	Burn-time (s)	Run.Fill numbers, test dates & comments
B	N	N	12.5	0.125	0.695	27.07	Supp7.11 (5/17/12)
B	N	N	25.0	0.250	1.611	44.03	Supp5.6 (5/11/12)
B	N	N	32.5	0.325	2.395	57.19	Supp7.10 (5/17/12)
B	N	Y/HX2	25.0	0.250	0.404	56.81	Supp6.8 (5/16/12)
B	N	Y/HX2	25.0	0.250	1.280	61.64	Supp6.9 (5/16/12); sequential burn
B	N	Y/HX2	12.5	0.125	0.191	20.39	Supp8.12 (5/18/12)
B	N	Y/HX2	32.5	0.325	0.593	74.26	Supp8.13 (5/18/12)
B	N	Y/HX2	50.0	0.500	3.527	78.80	Supp12.18 (6/7/12)
B	N	N	50.0	0.500	2.716	53.98	Supp14.21 (6/14/12); Initial P: 9 psi
B	N	N	25.0	0.250	0.706	94.44	Supp10.15 (5/22/12); Initial P: 6.5 psi

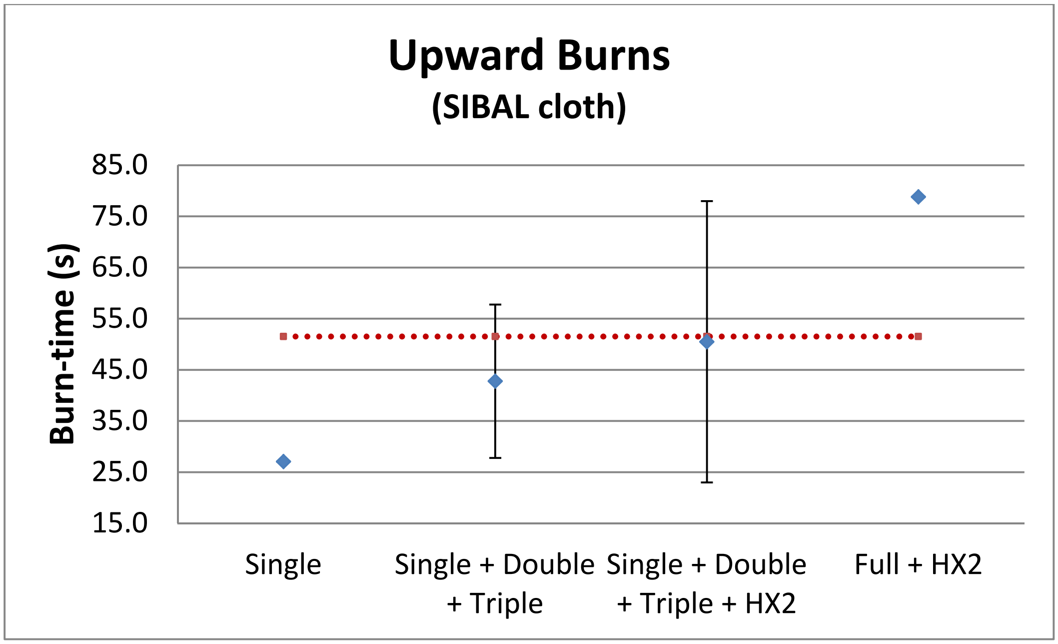

Figure 37.—Burn-times for SIBAL cloth upward burns.

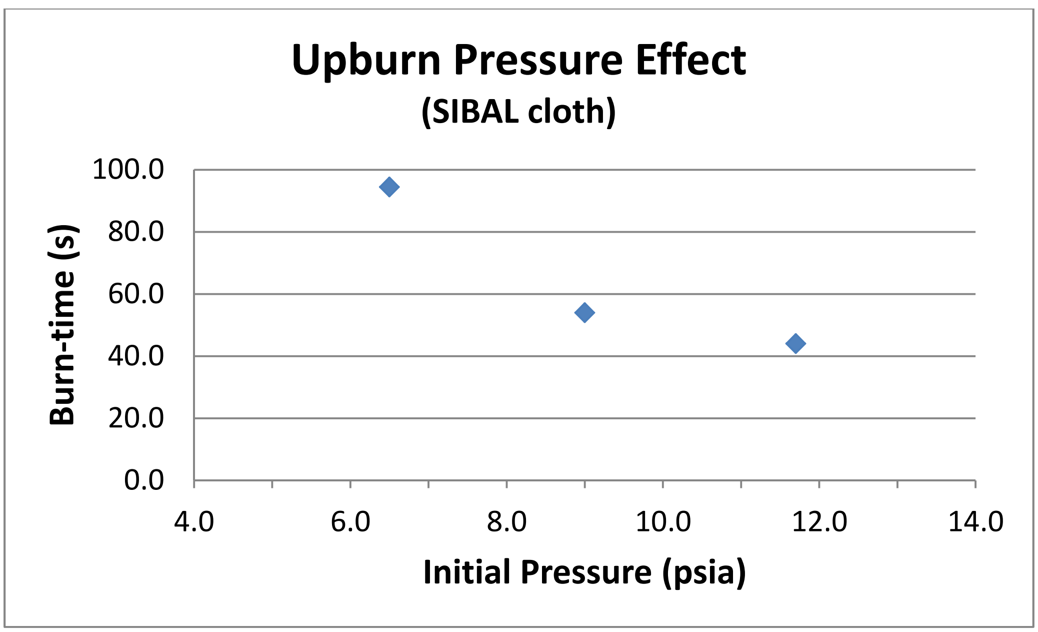

Figure 38.—SIBAL cloth upward burn pressure effect.

7.0 Closing Remarks

Given the quantity of test parameters and variants, gathering as much information as possible from as few experiments as possible became an immediate challenge. By utilizing a DOE approach to optimize the test matrix, the experiments were structured in a systematic mathematical fashion to aid in producing the most relevant and useful data output. The supplemental set of tests was motivated by the need to address additional parameters that were omitted from the DOE matrix generation for various reasons. Future publications will further convey the data relationships, trends, and correlations derived from the two matrices.

While recorded test details are captured in the test matrices listed in Appendix J, several details should be highlighted:

- While running top ignition (downward burn) cheesecloth tests, it was common to see an ember fall from the flame front and land a fraction of the way down the length of the sample, thus causing an upward burn. Several of these cases were noted as being "anomalous" and in some cases were included in the DOE as repeat tests.
- SIBAL tests with top ignition were attempted, but ignition could not be maintained.
- Smoke generation was greater when burning SIBAL fuel than when burning cheesecloth.
- Most of, if not all of, the tests that utilized the L2 heat exchanger were subject to smoke generation. A previously undisclosed protective coating was on the steel mesh and tended to smoke upon being heated beyond a certain (unknown) temperature.

If further testing is ever pursued to complement what has already been done, additional points of interest and value to both engineering and research include:

- Burning multi-layered fabric.
- Varying igniter power to determine min and max igniter power limits for a given sample material and igniter wire type.
- Examining additional starting pressure points.
- Varying oxygen concentration.
- Adding forced flow.
- Utilizing a heat exchanger with a similar mass to the L2 heat exchanger but with no coating.
- Filling the chamber with various materials with a variety of area/volume ratios placed at different locations to help characterize the heat transfer environment of the chamber for model validation purposes.

References

Kleinhenz, J., Ferkul, P., Pettegrew, R., Sacksteder, K., and T'ien, J.S. 2005. *One-sided Spread Phenomena of a Thermally Thin Composite Cotton/Fiberglass Fabric*. Fire and Materials, 29:27-37.

NASA, 2011, Kleinhenz, J., Yuan, Z., *An Experimental Study of Upward Burning Over Long Solid Fuels: Facility Development and Comparison*, NASA Technical Memo, NASA/TM—2011-217024.

Appendix A.—Experiment Operating Procedure

☐ Test director to review details on burning sequence with the test team.

☐ Verify igniter circuit with ohm meter.

☐ Extend anemometers to 1 in. from fuel card plane.

☐ Hook up igniter leads from fuel card to chamber feed through leads.
Only one igniter circuit should be hooked up on each panel. e.g., on panel #1 igniter circuit #1 top or igniter circuit #1 bottom should be hooked up, not both.

☐ Verify that all TCs have been extended to their proper positions.
For TC configuration A (without heat sink) TC6 is hooked to data channel 6.
For TC configuration D (with heat sink) TC9 is hooked to data channel 6.

☐ Turn ON all power supplies and TV monitors.

☐ Prepare Agilent Data Logger.

☐ Verify valid signals from thermocouples, anemometers, radiometers, and pressure transducers are being received by the data logger.

☐ Have crane crew prepare the chamber cap for installation.

☐ CONTINUOUS OPERATION REQUIRED BEYOND THIS POINT.

☐ Remove camera caps.

☐ Turn ON cameras: Open camera screens on HDR-CX110 cameras. Push ON buttons on HDR-XR160 cameras. (Screens on HDR-XR160 cameras will be open if HDMI cables are hooked up.)

☐ Verify that SD cards have been FORMATED to remove old video.

☐ Verify cameras FOV and that they are set for HD video. Review camera setup instruction sheet for other settings.

☐ KEEP A TIME LOG STARTING WITH THE TIME THE CAMERAS START RECORDING.

☐ Push RECORD on all four cameras. RECORD TIME.

☐ Install chamber cap. WATCH FOR CLEARANCE ON CAMERAS.

☐ Pump chamber down to 11.7 psia ±0.05 (~0.8 atmospheres) UNLESS DIRECTED OTHERWISE BY TEST DIRECTOR.

☐ Turn ON lights and verify camera views while chamber is pumping down.

☐ Turn OFF lights

☐ Push "PLAY" (▶) on the data logger.

☐ On the control box:

Igniter switch(s) for fuel panels to be burned ON
Igniter Enable ON
Confirm that all test team members are ready for the burn.
Push RED ON button and hold until ignition is visually confirmed using TV monitors.

NOTE: If sequential burns are to be performed turn OFF igniter switch on first panel as soon as ignition is confirmed, then turn ON igniter switch for second fuel panel. Push RED ON button as soon as first panel burn is complete. Follow same procedure for additional panels.

☐ Turn OFF lights at completion of burn. On short burns wait about one minute before turning lights off.

☐ At completion of burn:

Wait for temperature/pressure to decay for 10 min.
Turn fan ON for 5 min.
Turn fan OFF and allow chamber air to settle for 5 min.
Anemometer readings should be approaching zero.

☐ STOP data logger (■)

☐ Repeat above to burn additional panels.

☐ After final burn:

Turn OFF power supplies.
Purge chamber.
Remove chamber cap ASAP.
STOP cameras, download video, download data files, recharge batteries.
Vacuum chamber if necessary.

☐ Refer to fuel card removal and installation procedures to replace the fuel card.

Appendix B.—Experimental Rig Dimensions and Diagnostic Instrumentation Locations

The diagrams (Figs. 39 and 40) provide the overall experimental rack dimensions. Instrumentation locations relative to an XYZ coordinate system specified in Figure 41, are provided in Table 8.

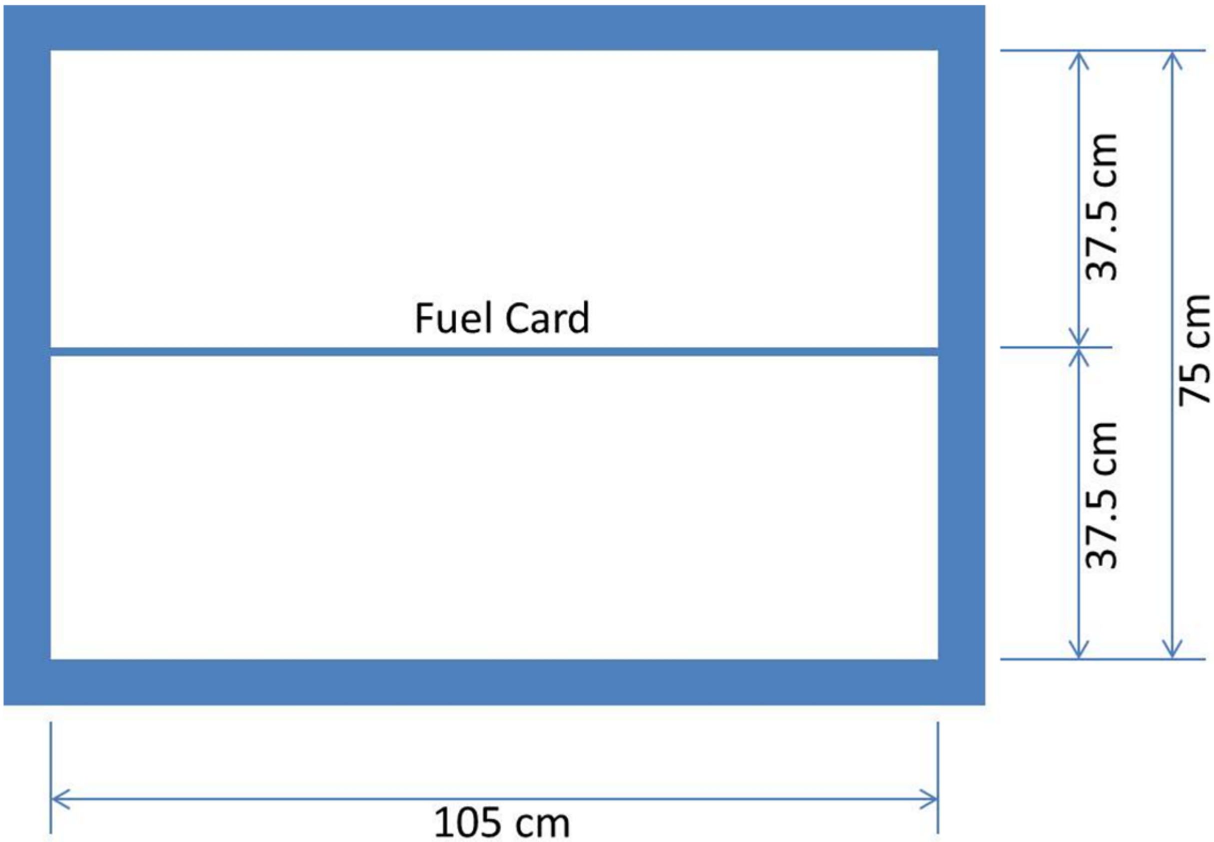

Figure 39.—Interior dimensions of the experimental frame (Top-view).

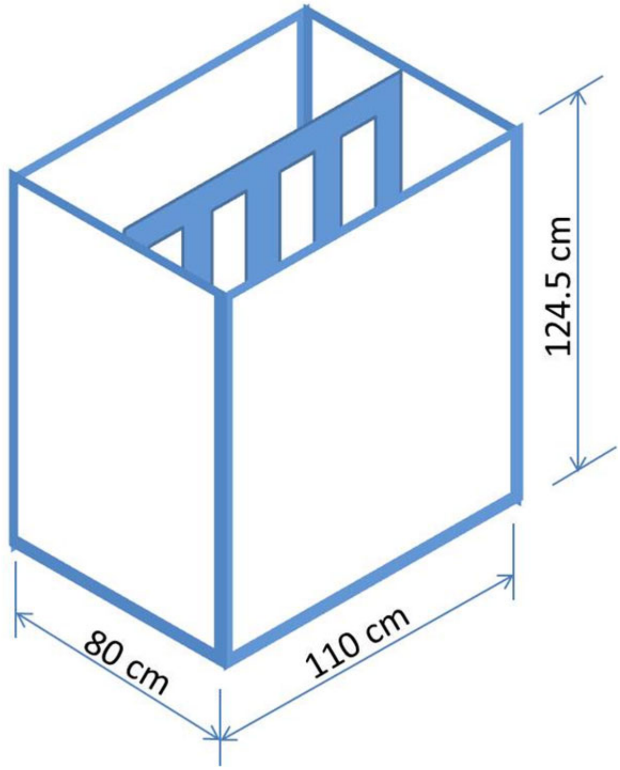

Figure 40.—External dimensions of combustion tunnel.

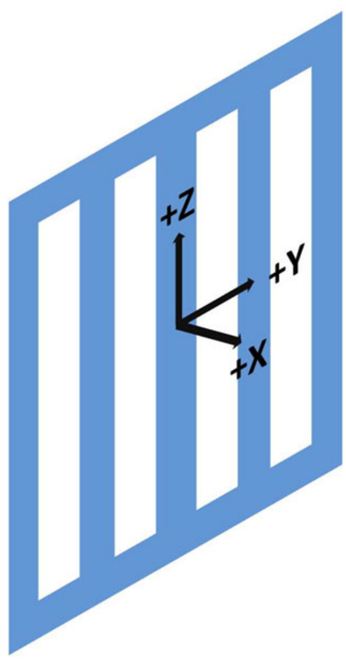

Figure 41.—Coordinate system used in Table 8.

TABLE 8.—DIAGNOSTIC INSTRUMENTATION LOCATIONS

Item	X coordinate	Y coordinate	Z coordinate
Camera HDR-XR160 Bottom	+53	0	–20
Camera HDR-XR160 Top	+53	0	+30
Camera HDR-CX110 Bottom	–50	0	–20
Camera HDR-CX110 Top	–50	0	+30
Radiometer 1 (Lower)	+38.75	0	–20
Radiometer 2 (Upper)	+38.75	0	+30
Anemometer 1 (Left)	+4	–12.5	–67
Anemometer 2 (Right)	+4	+12.5	–67
Thermocouple 1	+3	–37.5	+58
Thermocouple 2	+3	–12.5	+58
Thermocouple 3	+3	+37.5	+58
Thermocouple 4	–3	–31.7	+58
Thermocouple 5	–3	0	+58
Thermocouple 6 (Configuration A)	–3	+31.7	+58
Thermocouple 6 (Configuration D)	N/A	N/A	N/A
Thermocouple 7 (Configuration A)	0	0	+160
Thermocouple 7 (Configuration D)	0	–12.5	+160
Thermocouple 8	+3	+12.5	+58
Thermocouple 9 (Configuration D)	0	–12.5	+68
Note: Thermocouple 9 read out is on Thermocouple 6 data channel in Configuration D. Coordinate unit is centimeters.			

Note: The support post used for mounting Thermocouple 7 is not shown in the dimensioned diagram.

Appendix C.—As-Run Test Matrices

C.1. DOE Test Matrix, As-Run

The test matrix derived from the DOE is listed in Table 9. Unless otherwise stated in the matrix, the starting pressure for each run was approximately 11.7 psi (0.8 atmosphere). The material burned for all DOE tests was 90 grade bleached cheesecloth.

TABLE 9.—DOE TEST MATRIX, AS-RUN

Test/Fill number	Run	Width, cm	Area, m^2	Ignition location, Top/Bottom	Quench blocks, Yes/No	Heat exchanger, Yes/No	Comments		Test configuration details	Date
1	1	12.5	0.125	T	N	N	one sample		Thermocouple Configuration A.	4/5/2012
1	2	37.5	0.375	B	N	N	three sample simultaneous			
2	3	12.5	0.125	T	Y	N	one sample		Thermocouple Configuration A. The gain on the radiometers was adjusted before this test. The data may not be of great value or worth as a result. The gain was readjusted after this test and the radiometers were back to reading as they were during previous runs.	4/10/2012
2	4	12.5	0.375	B	N	N	three sample series	Start burning samples from left to right (as seen on HDR-XR160 cameras/"front "cameras).		
3	5	37.5	0.375	T	Y	N	three sample simultaneous		Thermocouple Configuration A.	4/16/2012
3	6	12.5	0.125	B	Y	N	one sample			
4	7	12.5	0.125	T	N	Y (L1)	one sample		Thermocouple Configuration B. (TC7 was moved from its location in Configuration A, approximately one meter above the top of the sample card, to approximately 2 in. above the HX material.) The HX material is approximately 1 in. thick (two 0.5 in. sheets stacked). The two aluminum honeycomb sheets weigh 380 g and 390 g.	4/17/2012
4	8	37.5	0.375	B	Y	Y (L1)	three sample simultaneous			

Test/Fill number	Run	Width, cm	Area, m^2	Ignition location, Top/Bottom	Quench blocks, Yes/No	Heat exchanger, Yes/No	Comments		Test configuration details	Date
5	9	12.5	0.125	T	N	Y (L1)	one sample		Thermocouple Configuration C. (TC7 was moved back to its original location and TC6 was moved to its place—approximately 2 in. above the HX material.)	4/19/2012
5	10	12.5	0.375	B	N	Y (L1)	three sample series	Start burning samples from left to right (as seen on HDR-XR160 cameras/"front "cameras).		
6	11	12.5	0.125	B	N	Y (L1)	one sample		Thermocouple Configuration C.	4/20/2012
6	12	37.5	0.375	T	Y	Y (L1)	three sample simultaneous			
7	13	12.5	0.125	B	N	N	one sample		Thermocouple Configuration A.	4/24/2012
7	14	37.5	0.375	T	N	N	three sample simultaneous			
8	15	12.5	0.125	T	Y	Y (L1)	one sample		Thermocouple Configuration D. (This configuration is most like Configuration C, except that the support arm that TC6 is attach to was rotated to a position above the HX directly across from TC2.)	4/26/2012
8	16	37.5	0.375	B	N	Y (L1)	three sample simultaneous			
9	17	12.5	0.125	B	Y	Y (L1)	one sample		Thermocouple Configuration D. During run 18, the center sample shed a small ember which hit close to halfway down the length of the sample and caused a brief upward burn of that sample area. Test may need to be re-run due to this anomaly.	4/30/2012
9	18	37.5	0.375	T	N	Y (L1)	three sample simultaneous			
10	19	12.5	0.125	B	N	N	one sample	Repeat of Test 7, Run 13 on 04/24/2012.	Thermocouple Configuration A. This was the first test that was run with the black cardstock/cardboard	5/2/2012

Test/Fill number	Run	Width, cm	Area, m^2	Ignition location, Top/Bottom	Quench blocks, Yes/No	Heat exchanger, Yes/No	Comments		Test configuration details	Date
10	20	12.5	0.375	T	Y	N	three sample series	Start burning samples from left to right (as seen on HDR-XR160 cameras/"front "cameras).	on the back side of the experimental rig to prevent the LED reflection in the HD-160 camera view.	
11	21	12.5	0.125	B	Y	N	one sample	Repeat of Test 3, Run 6 on 04/16/2012.	Thermocouple Configuration A. During run 22, the center sample shed a small ember which hit about 10 cm from the top of the sample, causing upward burning.(Upon removal of the sample card, two TCs, 5 and 6, were slightly jarred when the sample card bowed. They were verified as still properly functioning.)	5/3/2012
11	22	12.5	0.375	T	N	N	three sample series	Start burning samples from left to right (as seen on HDR-XR160 cameras/"front "cameras).		
12	23	12.5	0.125	T	Y	N	one sample	Repeat of Test 2, Run 3 on 04/10/2012.	Thermocouple Configuration A. During run 23, the sample shed a small ember which fell and hit just a couple centimeters below the top of the sample causing upward burning.	5/4/2012
12	24	12.5	0.375	B	Y	N	three sample series	Start burning samples from left to right (as seen on HDR-XR160 cameras/"front "cameras).		
13	25	12.5	0.125	B	Y	Y (L1)	one sample	Repeat of Test 9, Run 17 on 04/30/2012.	Thermocouple Configuration D. During rerun 18, the sample on the right (as viewed from the HX-160 cameras) shed a small ember which fell and hit about one quarter of the distance from the top of the sample causing upward burning.	5/7/2012
13	26	37.5	0.375	T	N	Y (L1)	three sample simultaneous	Repeat of Test 9, Run 18 on 04/30/2012.		
14	27	12.5	0.125	B	N	Y (L1)	one sample	Repeat of Test 6, Run 11 on 04/20/2012.	Thermocouple Configuration D.	5/9/2012

Test/Fill number	Run	Width, cm	Area, m^2	Ignition location, Top/Bottom	Quench blocks, Yes/No	Heat exchanger, Yes/No	Comments		Test configuration details	Date
14	28	12.5	0.375	B	Y	Y (L1)	three sample series	Start burning samples from left to right (as seen on HDR-XR160 cameras/"front "cameras).		
15	29	12.5	0.125	T	Y	Y (L1)	one sample	Repeat of Test 8, Run 15 on 04/26/2012.	Thermocouple Configuration D.	5/10/2012
15	30	12.5	0.375	T	N	Y (L1)	three sample series	Start burning samples from left to right (as seen on HDR-XR160 cameras/"front "cameras).		
16	31	12.5	0.125	T	N	Y (L2)	one sample		Thermocouple Configuration D. “New” heat exchanger (L2).	5/23/2012
16	32	12.5	0.375	B	N	Y (L2)	three sample series	Start burning samples from left to right (as seen on HDR-XR160 cameras/"front "cameras).		
17	33	12.5	0.125	B	N	Y (L2)	one sample		Thermocouple Configuration D. “New” heat exchanger (L2).	5/24/2012
17	34	37.5	0.375	T	N	Y (L2)	three sample simultaneous			
18	35	12.5	0.125	B	Y	Y (L2)	one sample		Thermocouple Configuration D. “New” heat exchanger (L2).	5/25/2012
18	36	37.5	0.375	B	Y	Y (L2)	three sample simultaneous			
19	37	12.5	0.125	T	Y	Y (L2)	one sample		Thermocouple Configuration D. “New” heat exchanger (L2).	5/29/2012

Test/Fill number	Run	Width, cm	Area, m^2	Ignition location, Top/Bottom	Quench blocks, Yes/No	Heat exchanger, Yes/No	Comments		Test configuration details	Date
19	38	12.5	0.375	T	Y	Y (L2)	three sample series	Start burning samples from left to right (as seen on HDR-XR160 cameras/"front "cameras).		
20	39	12.5	0.375	T	N	N	three sample series	Start burning samples from left to right (as seen on HDR-XR160 cameras/"front "cameras). Originally run on 5/3/2012 (Fill 11/Run22).	Thermocouple Configuration A.	5/30/2012
20	40	12.5	0.125	T	Y	N	one sample	Original run on 4/10/2012 (Fill2/Run3) was fine, but the replicate run on 5/4/2012 (Fill 12/Run 23) was anomalous.		
21	41	37.5	0.375	T	N	Y (L1)	three sample simultaneous	Originally run on 4/30/2012 (Fill9/Run18); retest (Fill 13/Run 26) on 5/7/2012 was also anomalous.	Thermocouple Configuration D.	5/31/2012

Test/Fill number	Run	Width, cm	Area, m^2	Ignition location, Top/Bottom	Quench blocks, Yes/No	Heat exchanger, Yes/No	Comments		Test configuration details	Date
21	42	12.5	0.125	B	N	Y (L1)	one sample	Replicate of Fill 6/Run 11 on 4/20/2012 and Fill 14/Run 27 on 5/9/2012.		
22	43	37.5	0.375	T	N	N	three sample simultaneous	Repeat of "suspicious" Fill 7/Run 14 on 4/24/2012.	Thermocouple Configuration A.	6/1/2012
22	44	12.5	0.125	B	N	N	one sample	Replicate of Fill 7/Run 13 on 4/24/2012 and Fill 10/Run 19 on 5/2/2012.		
23	45	37.5	0.375	T	Y	N	three sample simultaneous	Repeat of "suspicious" Fill 3/Run 5 on 4/16/2012.	Thermocouple Configuration A.	6/4/2012
23	46	12.5	0.125	B	N	N	one sample	Replicate of Fill 7/Run 13 on 4/24/2012, Fill 10/Run 19 on 5/2/2012 and Fill 22/Run 44 on 6/1/2012.		

.

C.2 Supplementary Test Matrix, As-Run

The supplemental tests run in addition to the tests in the DOE matrix are listed in Table 10. Unless otherwise stated, the starting pressure for each run was approximately 11.7 psi (0.8 atmosphere).

TABLE 10.—SUPPLEMENTARY TEST MATRIX, AS-RUN

Test/Fill number	Run	Width, cm	Area, M^2	Ignition location, Top/Bottom	Quench blocks, Yes/No	Heat exchanger, Yes/No	Comments		Test configuration details	Date
*1	1	25	0.25	B	N	N	two sample simultaneous	cheesecloth	Thermocouple Configuration A.	3/29/2012
*1	2	12.5	0.25	B	N	N	two sample sequential	cheesecloth		
2	3	50	0.5	T	N	N	large sample	cheesecloth	Thermocouple Configuration A. 15 cm igniter.	4/27/2012
3	4	50	0.5	B	N	N	large sample	cheesecloth	Thermocouple Configuration A. 15 cm igniter.	5/1/2012
4	5	50	0.5	B	N	N	large sample	cheesecloth	Thermocouple Configuration A. Full bottom width ignition.	5/3/2012
5	6	25	0.25	B	N	N	two sample simultaneous	SIBAL	Thermocouple Configuration A. Run 2 failed to ignite from the top. The chamber was opened and the sample material was reconfigured so the run could be re-executed. The retest failed to maintain ignition again.	5/11/2012
5	7	25	0.25	T	N	N	two sample simultaneous	SIBAL		
6	8	25	0.25	B	N	Y (L2)	two sample simultaneous	SIBAL	Thermocouple Configuration D. The sampler closest to the middle of the sample holder seemed to finish burning after the first sample even though the two were ignited simultaneously. Once the burning was complete, the test enclosure filled with smoke, which was expected to have happened due to the presence of	5/16/2012

Test/Fill number	Run	Width, cm	Area, M^2	Ignition location, Top/Bottom	Quench blocks, Yes/No	Heat exchanger, Yes/No	Comments		Test configuration details	Date
6	9	12.5	0.25	B	N	Y (L2)	two sample series	SIBAL	the heat exchanger and no forced air flow. The smoke did not clear out during the quiescent periods or during fan operation, therefore in order to achieve meaningful visual data, the chamber was pumped down to approx. 8 psi before Run 4 and air was vented. Once reasonable clarity was achieved, Run 4 was executed. The test enclosure filled with smoke a second time following Run 4.	
7	10	37.5	0.375	B	N	N	three sample simultaneous	SIBAL	Thermocouple Configuration A. Smoke was not evident during the test, but after the test was completed and after the chamber was vented. When the cap was removed there was still smoke within the chamber.	5/17/2012
7	11	12.5	0.125	B	N	N	one sample	SIBAL		
8	12	12.5	0.125	B	N	Y (L2)	one sample	SIBAL	Thermocouple Configuration D. Before this test was executed, the heat exchanger panels were heated with a flame outside of the chamber in an attempt to burn off a suspected coating which was thought to be contributing to the smoke generation during SIBAL testing. The decision was made to burn one strip first to see how much smoke would be generated. The smoke did not seem overly significant so the second run burning 3 strips was executed. The three strip burn produced less than or equal to (at least visually) the amount of smoke created during SIBAL Test 2.	5/18/2012
8	13	37.5	0.375	B	N	Y (L2)	three sample simultaneous	SIBAL		

Test/Fill number	Run	Width, cm	Area, M^2	Ignition location, Top/Bottom	Quench blocks, Yes/No	Heat exchanger, Yes/No	Comments		Test configuration details	Date
9	14	50	0.5	B	N	N	large sample burn	cheesecloth, 15 cm igniter, 6.5 psi (approx. 0.45 atm).	Thermocouple Configuration A.	5/21/2012
10	15	25	0.25	B	N	N	two sample simultaneous	SIBAL, positions 3 and 4, 6.5 psi (approx. 0.45 atm).	Thermocouple Configuration A. SIBAL samples were burned first. The flame on the sample in position 3 seemed to burn out and leave some material behind. However, the material still must have burned without a noticeable flame present because the material that remained, “disappeared”.	5/22/2012
10	16	25	0.25	B	N	N	two sample simultaneous	cheesecloth, positions 1 and 2 (approx. 0.45 atm).		
11	17	50	0.5	B	N	Y (L2)	large sample	cheesecloth, full width igniter, 11.7 psi (approx. 0.8 atm).	Thermocouple Configuration D.	6/6/2012
12	18	50	0.5	B	N	Y (L2)	large sample	SIBAL, full width igniter, 11.7 psi (approx. 0.8atm)	Thermocouple Configuration D. During the experiment the heat exchanger did a great job absorbing the heat generated by the burn and kept the pressure down. However, once the sample neared burning completion the heat exchanger was ignited by the sample flame. It’s ignition was evident by the flickering visible on the video feed and by the sudden jump in pressure. The pressure went above atmospheric and popped the chamber relief.	6/7/2012
13	19	25	0.25	B	N	N	two sample simultaneous	cheesecloth, 5 psi	Thermocouple Configuration A.	6/8/2012
13	20	25	0.25	B	N	N	two sample simultaneous	cheesecloth, 9 psi		

*Note: While listed in the Supplementary Test Matrix, Test 1, Runs 1 and 2, were included in the DOE Response Model evaluation.

Appendix D.—Initial Experimental Rig Concept

Figure 42 is the initial conceptual sketch of the experimental rig. This sketch provided the basis for the engineering drawings of the sample cards and the overall experiment structure.

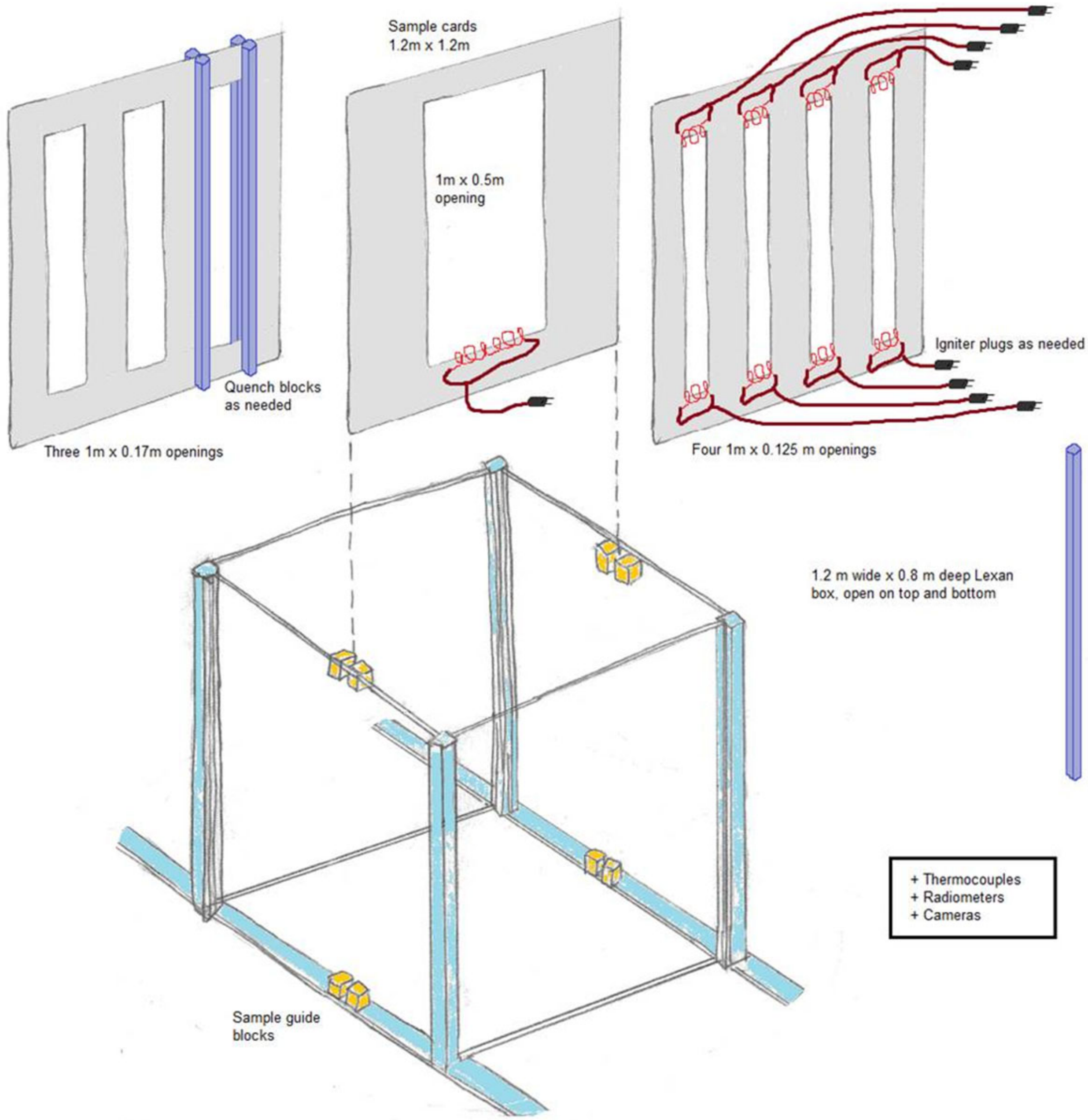

Figure 42.—Sketch of initial experimental rig concept.

Appendix E.—Engineering Drawings

The following engineering drawings, Figures 43 to 46, were produced for the fabrication of the thermocouple support plate, which was the bar used for mounting the thermocouples, and the three sample cards. Only two out of the three sample card designs that were fabricated were used for testing.

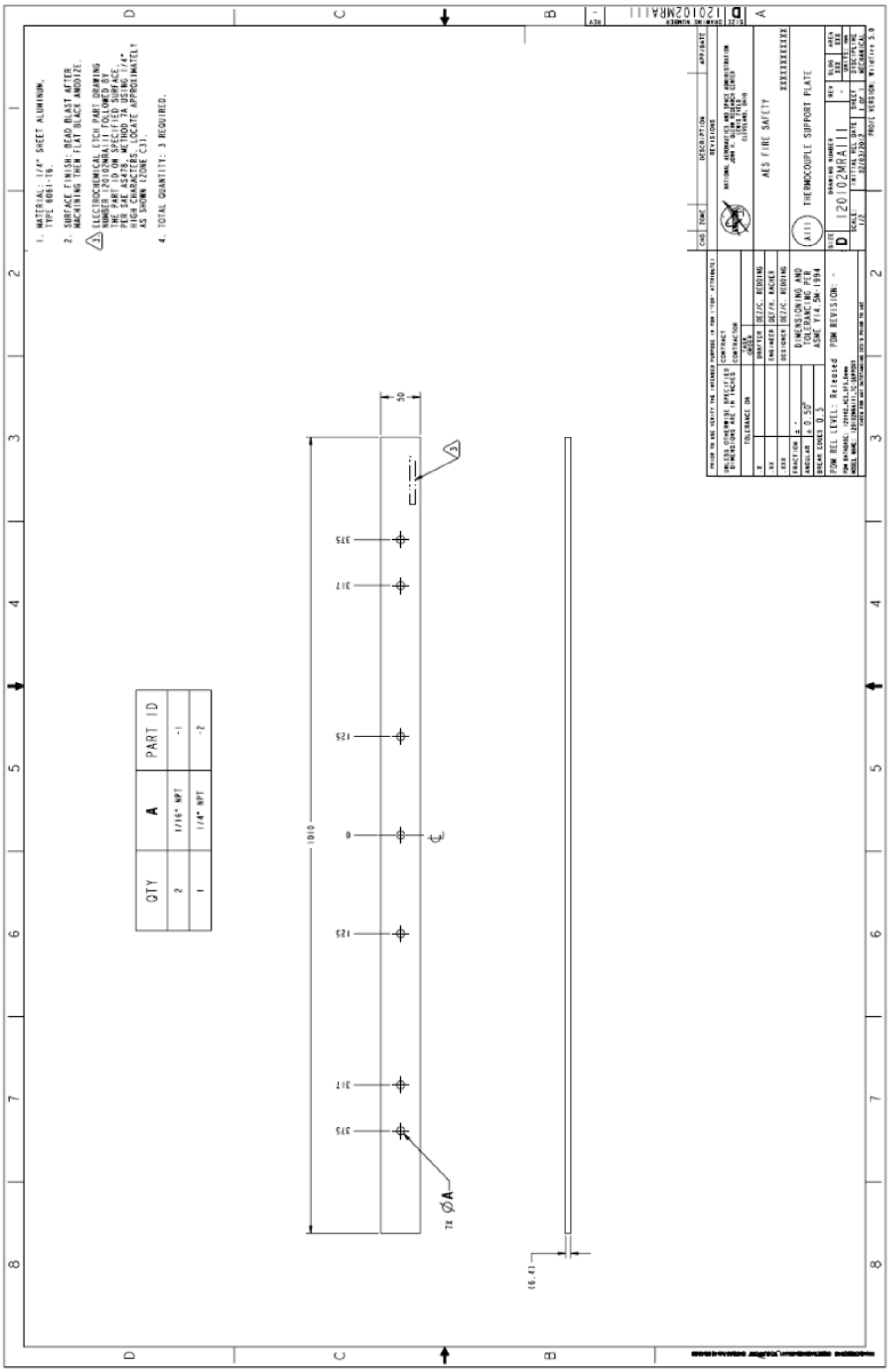

Figure 43.—Thermocouple Support Plate Drawing.

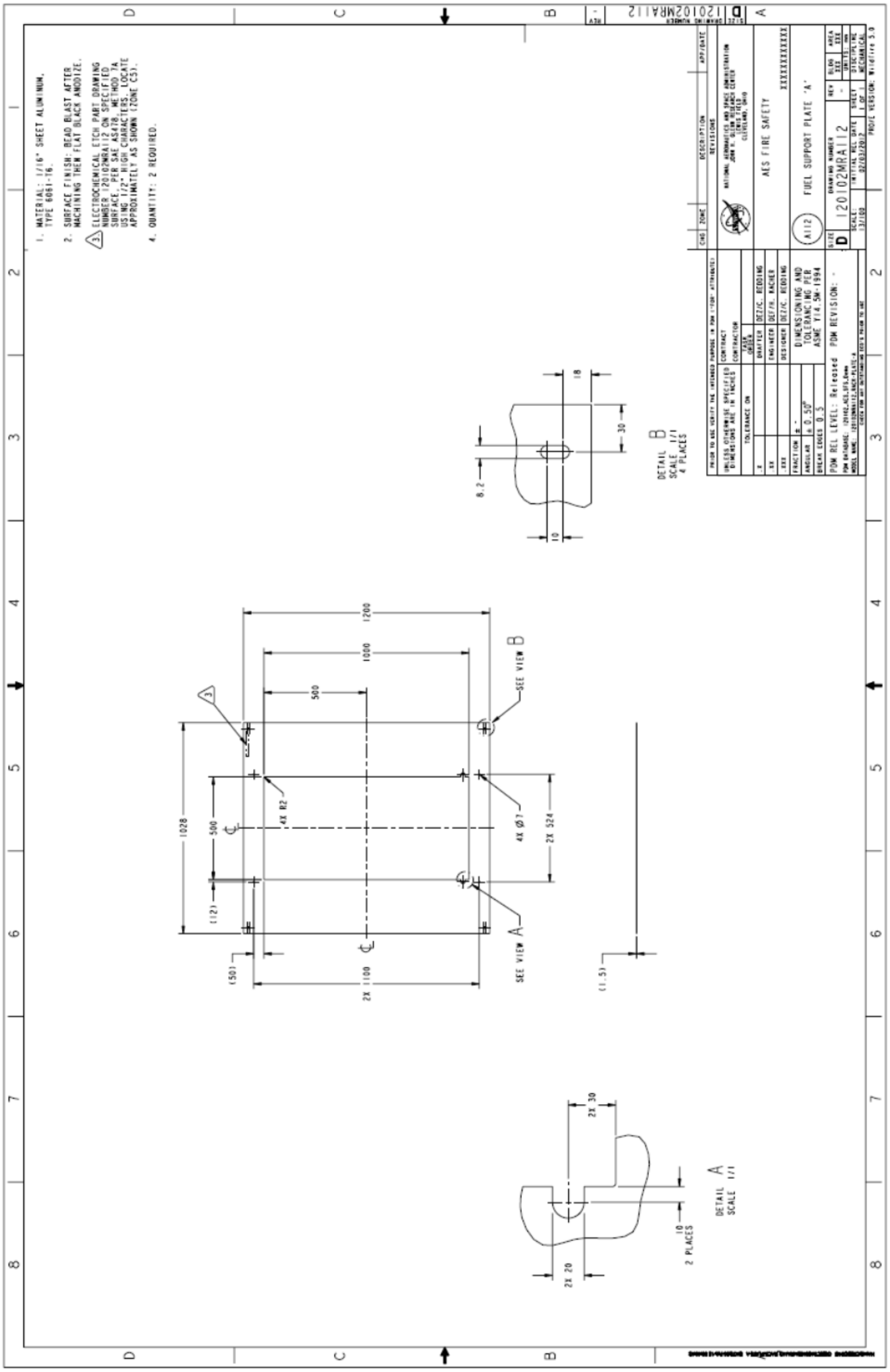

Figure 44.—One slot, 50 by 100 cm, sample holder drawing.

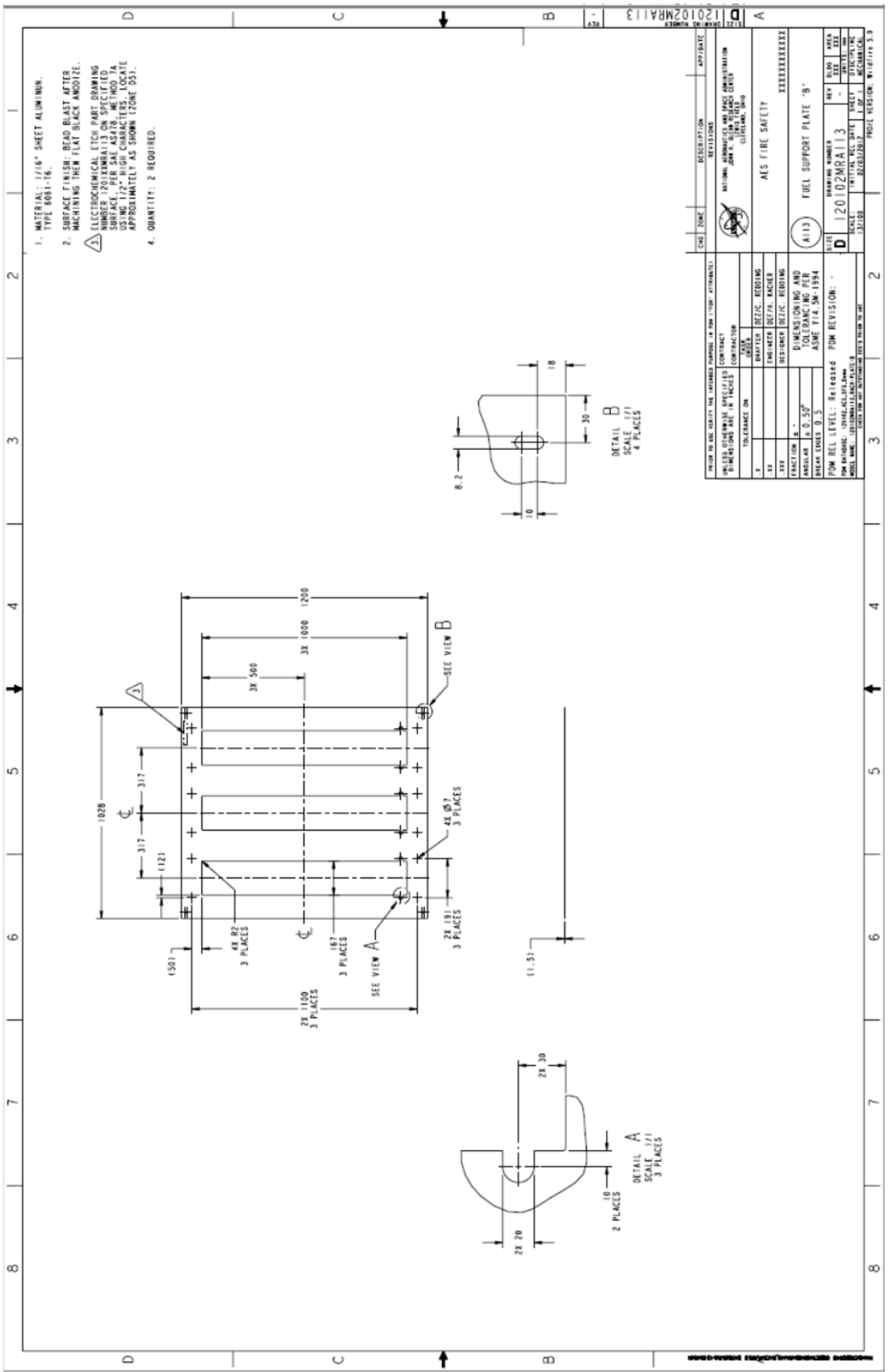

Figure 45.—Three slot, 16.7 by 100 cm, sample holder drawing.

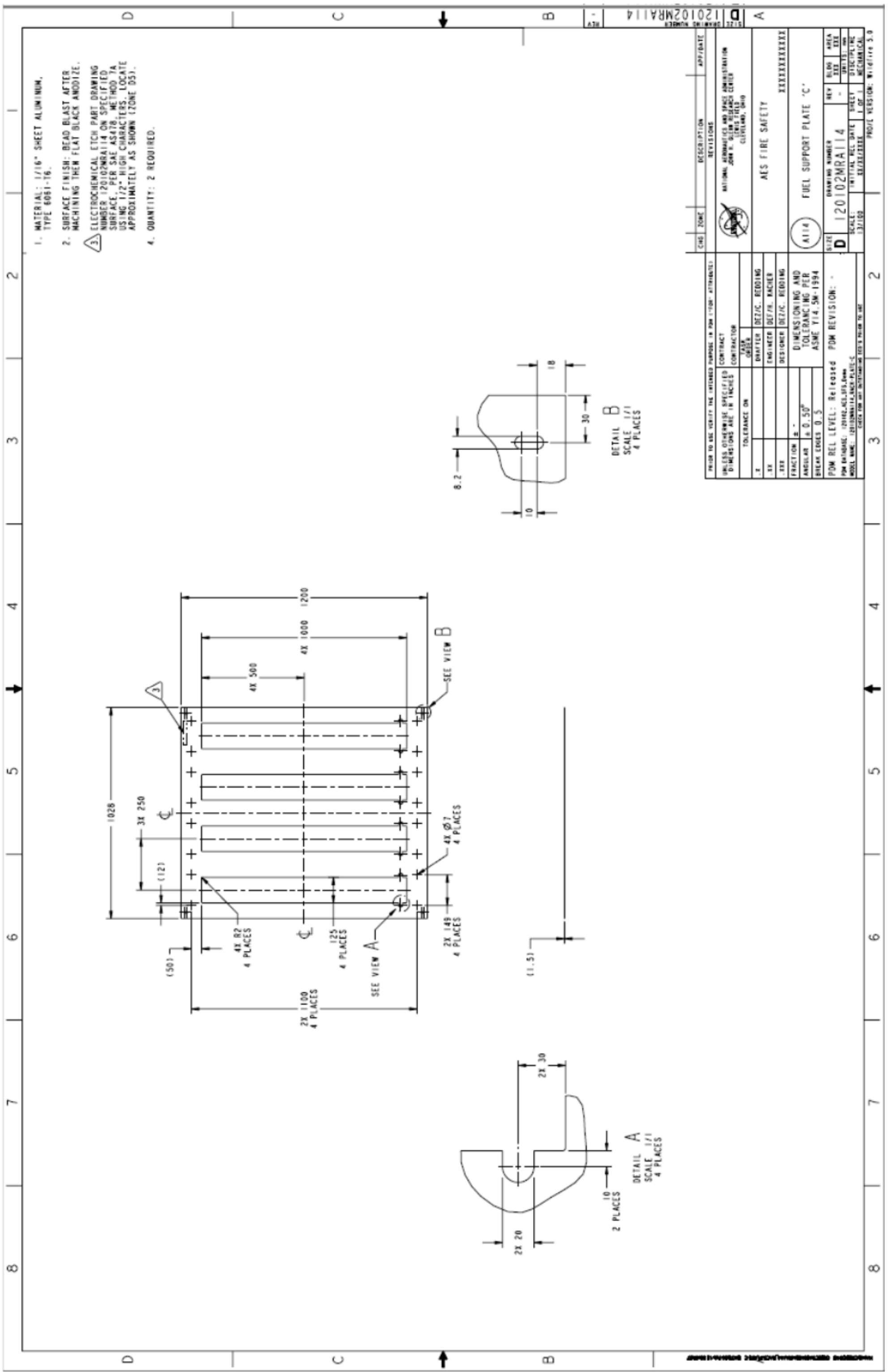

Figure 46.—Four slot, 12.5 by 100 cm, sample holder drawing.

Appendix F.—Sample Holder Installation Procedure

☐ Position ladder to provide access to top of frame in the vacuum chamber. NOTE: Ladder may have to be repositioned for various phases of the sample holder (fuel card) installation.

☐ Loosen pivot on upper thermocouple (#7) support arm and rotate arm 90° to provide clearance over center of the frame duct area.

☐ Unscrew nut(s) on fitting(s) holding thermocouple(s) in center position and back thermocouple(s) out as far as possible, This is required to prevent clevis on fuel card from damaging thermocouples.

☐ Position crane on EAST side of chamber. North/South position of crane from chamber lid removal should not be changed.

☐ Verify proof dates on a clevis and sling to be used to install the fuel card. Fuel card will weigh from 10 to 30 lb

☐ Mount fuel card to crane using sling and clevis. Check with test director whether the fuel card igniters are to be at the top or bottom. Igniter connectors must be at EAST corner of fuel card. Clevis pin head must face away from the center thermocouple (normally NORTH). TAPE CLEVIS TO SLING TO PREVENT IT FROM FALLING OFF IN A LATER STEP.

☐ Lift fuel card until card bottom is above the top of the frame.

☐ A person needs to be on the ladder positioned next to the chamber such that they will not interfere with westward movement of the fuel card.

☐ Slowly move the fuel card WEST while the person on the ladder guides the fuel card until it is centered over the frame.

☐ Slowly lower the fuel card while guiding it into the channels on the frame. EXTREME CAUTION MUST BE EXERCISED DURING THIS OPERATION TO PREVENT CONTACT WITH THE THERMOCOUPLES BY THE FUEL CARD OR THE CLEVIS.

☐ When the fuel card is seated CAREFULLY remove the pin from the clevis and lift the clevis clear of the frame.

☐ Move center thermocouple(s) back into position and snug nut(s).
CAUTION - OVER TIGHTENING NUTS MAY DAMAGE THE THERMOCOUPLE.

☐ Re-center upper thermocouple (#7) over fuel card.

☐ Connect igniter leads (1, 3, or 4 leads depending on fuel card being used) on EAST corner of fuel card.

Appendix G.—Sample Holder Removal Procedure

☐ Position ladder to provide access to top of frame in the vacuum chamber. NOTE: Ladder may have to be repositioned for various phases of the sample holder (fuel card) removal.

☐ Loosen pivot on upper thermocouple (#7) support arm and rotate arm 90° to provide clearance over center of the frame duct area.

☐ Unscrew nut(s) on fitting(s) holding thermocouple(s) in center position and back thermocouple(s) out as far as possible, This is required to prevent clevis on fuel card from damaging thermocouples.

☐ Disconnect igniter leads (1, 3, or 4 leads depending on fuel card being used) on EAST corner of fuel card.

☐ Position crane on EAST side of chamber. North/South position of crane from chamber lid removal should not be changed.

☐ Verify proof dates on a clevis and sling to be used to install the fuel card. Fuel card will weigh from 10 to 30 lb

☐ Mount sling and clevis on crane hook with clevis pin head facing away from center thermocouple. Remove clevis pin. TAPE CLEVIS TO SLING TO PREVENT IT FROM FALLING OFF IN A LATER STEP.

☐ Move crane WEST to center lift sling/clevis over the fuel card.

☐ A person needs to be on the ladder positioned next to the chamber to guide the clevis to the proper location and insert the pin.

☐ Slowly lower the crane hook while the person on the ladder guides the clevis to the proper location. EXTREME CAUTION MUST BE EXERCISED DURING THIS OPERATION TO PREVENT CONTACT WITH THE THERMOCOUPLES BY THE CLEVIS.

☐ When the clevis is in the proper location insert the pin through the clevis and hole in the upper center of the fuel card.

☐ Slowly lift the fuel card with the crane while the person on the ladder guides the fuel card. When clear of the frame move the fuel card EAST and lower to floor level for removal from the clevis.

☐ The center thermocouple(s) and the upper thermocouple can remain in their retracted positions until after another fuel card is installed.

Appendix H.—Camera Settings

Camera settings were adjusted to suit the needs of the video documentation and are captured in Tables 11 and 12. Several settings on the Sony HDR-CX110 cameras required resetting prior to each test and are highlighted in Table 12 accordingly.

TABLE 11.—CAMERA SETTINGS FOR XR160

SONY HDR-XR160	
Select appropriate icon to make settings	
Shooting Mode	
Movie	
Camera/mic	
Manual Settings	
White Balance	Outdoor
Spot Meter Focus	Manual
Spot Meter	Manual
Spot Focus	Manual
Exposure	Manual
Focus	.1m
Low Lux	ON
Fader	OFF
Telemacro	OFF
Steady Shot	Active
Digital Zoom	OFF
Conversion Lense	Wide Conversion
Autobacklight	OFF
Smile Sensitivity	Normal smile
Built in Zoom Mic	OFF
Wind Noise Red:	OFF
Audio Mode	5.1 ch surround
Mic Ref Level	Normal
Guideframe	OFF
Display Setting	OFF
Audio Level Display	OFF
Image Qual/Size	
Rec Mode	Highest Qual FX
Frame Rate	60i
HD/STD Setting	HD Quality
XV Color	ON
Playback Function	
N/A	
Edit Function	
N/A	
Media Settings	
Media Select	Memory Card
Media Info	N/A
Forman	N/A
Repair img DFB	N/A
File Number	Series

(yellow)	Essential Settings
(pink)	**Always require reset before each test**

TABLE 12.—CAMERA SETTINGS FOR CX110

SONY HDR-CX110	
Choose "Select Others" on the Main Menu to make all appropriate settings	
Manual Settings	
Scene Selection	Auto
Fader	N/A
White Balance	Outdoor
Spot mtr/fcs	Auto
Spot Meter	Auto
Spot Focus	Auto
Exposure	Auto
Telemacro	OFF
Smthslow rec	N/A
Shooting Settings	
HD/STD set	HD
Record Mode	HDFX
Guideframe	OFF
Steady Shot	Active
Conversion Lense	Wide Conversion
Low Lux	ON
Face Detection	OFF
Priority Setting	NA
Smile Detection	NA
Smile Sensitivity	NA
Audio Rec Set	
Built in Zoom Mic	OFF
Mic Ref Level	Normal
Other rec set	
Digital zoom	OFF
Auto backlight	OFF
XV color	ON
Photo Settings	
Self Timer	N/A
Image Size	3.1m
File No.	Series
Playback Settings	
N/A	
Edit Settings	
N/A	
Other Settings	
N/A	
Manage Media	
N/A	
General Settings	
Set Clock	

Appendix I.—Thermocouple Diagrams

Throughout testing, several different iterations of thermocouple configurations were used in an effort to achieve a configuration suitable for capturing the temperature delta across the heat exchanger. The thermocouple diagrams can be referred to when evaluating the thermocouple data from a specific test fill and run.

Thermocouple Configuration A—This is the standard thermocouple configuration used for all tests without a heat exchanger (Fig. 47).

Thermocouple Configuration B—This configuration was used for the first test that utilized a heat exchanger. The thermocouple in the upper chamber was moved downward so that it was approximately 2 in. above the heat exchanger (Fig. 47).

Thermocouple Configuration C—This configuration resulted from the desire to maintain a temperature reading in the upper chamber volume. Thermocouple 6 was moved to a position less than 2 in. from the top of the heat exchanger (Fig. 48).

Thermocouple Configuration D—This configuration resulted from the desire to yield a temperature delta across the heat exchanger at a location centered above one of the four slotted sample cards. Notice that this configuration differs from “C” in that Thermocouple 6 is angled to be above the heat exchanger opposite Thermocouple 2 (Fig. 48).

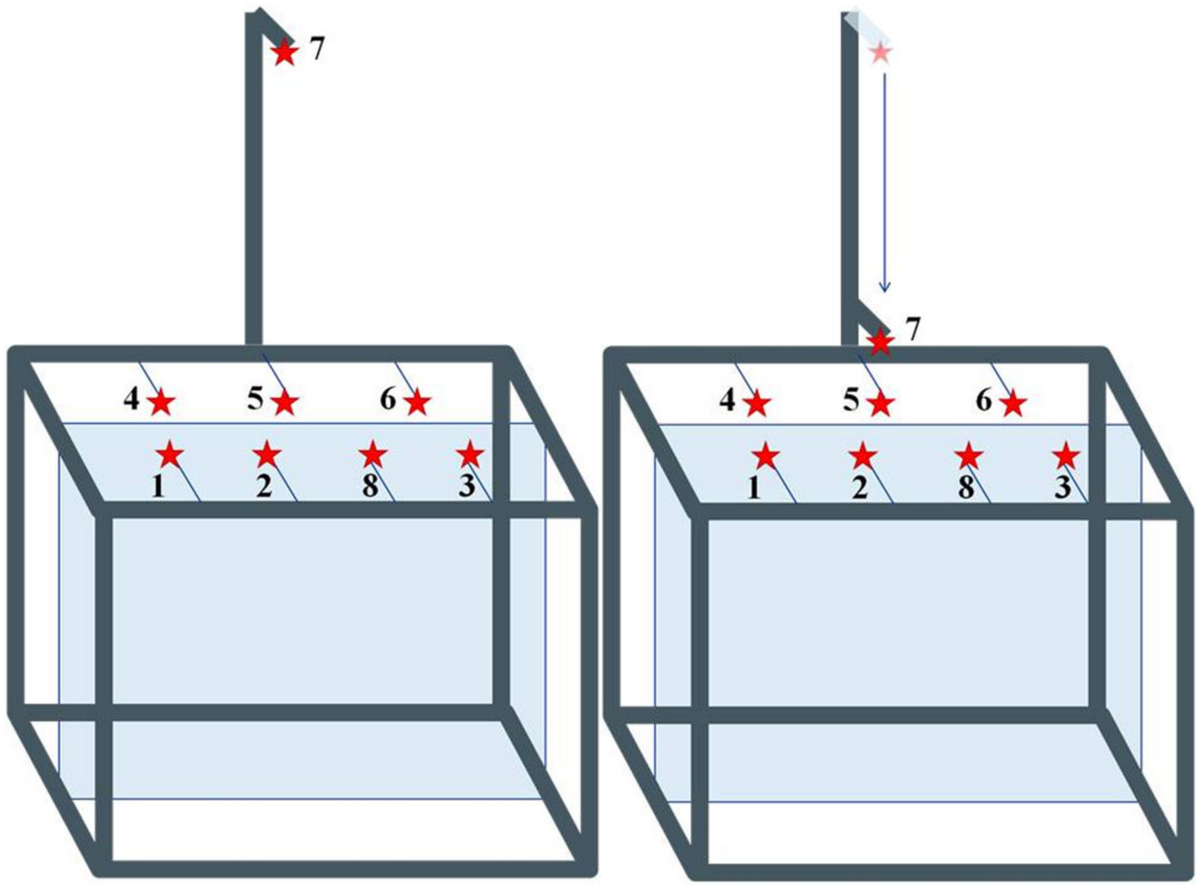

Thermocouple Configuration A Thermocouple Configuration B

Figure 47.—Thermocouple configurations A and B.

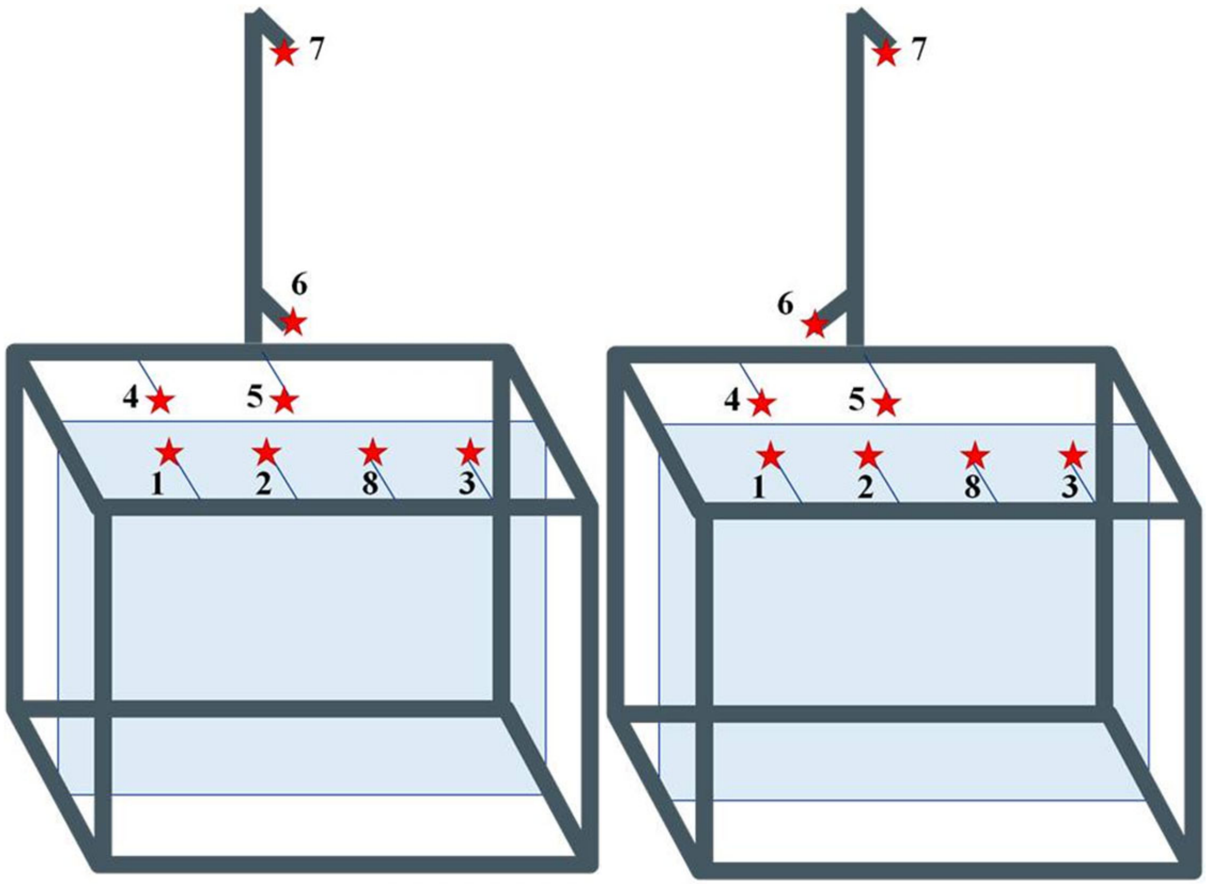

Thermocouple Configuration C Thermocouple Configuration D

Figure 48.—Thermocouple configurations C and D.

Appendix J.—Agilent Data-Logger Instructions

1) AT DATA LOGGER: If not already powered up, press the power button on the Agilent 34980A DAQ to power it up. Give the unit time to initialize before activating the software.
2) AT COMPUTER: Activate the Agilent Bench-Link Pro Data Logger software. (Icon is near middle of desktop screen)
3) The software will initialize itself and connect to the DAQ. Once up, select one of the last 4 tabs on the screen:

   QUICK GRAPH—Displays graphs and numeric values for the two radiometers and the igniter "on" signal (RAD_TOP, RAD_BOT, IGN_ACT)

   GRAPH 2—Displays graphs and numeric values for the two anemometers and the two pressure transducers (ANEM_1, ANEM_2, 0-20_PSIA, 0-25_PSIA)

   GRAPH 3—Displays graphs and numeric values for the first four thermocouples (TC1, TC2, TC3, TC4)

   GRAPH 4—Displays graphs and numeric values for the last four thermocouples (TC5, TC6, TC7, TC8)

4) To initiate data logging, click the PLAY (arrow/triangle) button near top middle of the screen. Shortly after, clicking noises will be coming out of the DAQ and the screen display graphs will begin updating. Use the tabs to observe the desired output signals.
5) To stop the logging process, simply click on the stop (square) button near the top middle of the screen. When logging is stopped, the data file is automatically exported to a comma-delimited file into the VF-13 AES Data folder. A shortcut link to this folder is located near the middle of the desktop screen. It is a .csv file that can be opened directly by Microsoft Excel.
6) A thumbdrive can be used to off load the files.

Appendix K.—Final DOE With Experimental and Response Model Delta P

The experimental results for Delta P (calculated and verified) and the response model predicted Delta P can be found in Table 13. Dates in the comments section can be cross referenced with the as-run DOE test matrix.

TABLE 13.—FINAL DOE WITH EXPERIMENTAL AND RESPONSE MODEL DELTA P

	Ignition Location	Quench Block	Heat Exchanger	FES Width	FES Area	Delta P	Comments	Response Model Delta P
1	T	Y	N	12.5	0.375	0.149	10.20 (5/2/12), FES7	0.199
2	T	N	N	12.5	0.375	0.161	11.22 (5/3/12), FES7, Anomaly	0.179
3	B	N	N	12.5	0.125	0.442	7.13 (4/24/12), FES1	0.475
4	B	Y	N	12.5	0.125	0.394	3.6 (4/16/12), FES1	0.395
5	B	Y	N	12.5	0.375	0.859	12.24 (5/4/12), FES7	0.890
6	T	Y	N	12.5	0.125	0.13	2.3 (4/10/12), FES1	0.090
7	B	N	N	12.5	0.375	1.051	2.4 (4/10/12), FES7	0.988
8	T	Y	N	37.5	0.375	0.275	3.5 (4/16/12), FES3	0.259
9	T	N	N	37.5	0.375	0.337	7.14 (4/24/12), FES3	0.377
10	B	N	N	37.5	0.375	1.369	1.2 (4/5/12), FES3	1.296
11	B	Y	L1	12.5	0.125	0.294	9.17 (4/30/12), FES1	0.293
12	T	Y	L1	12.5	0.125	0.118	8.15 (4/26/12), FES1	0.150
13	T	N	L1	12.5	0.375	0.164	15.30 (5/10/12), FES7	0.186
14	T	N	L1	12.5	0.125	0.129	4.7 (4/17/12), FES1	0.082
15	B	Y	L1	12.5	0.375	0.759	14.28 (5/9/12), FES7	0.765
16	B	N	L1	12.5	0.125	0.334	6.11 (4/20/12), FES1	0.343
17	T	Y	L1	37.5	0.375	0.281	6.12 (4/20/12), FES3	0.255
18	T	N	L1	37.5	0.375	0.315	9.18 (4/30/12), FES3, Anomaly	0.342
19	B	N	L1	37.5	0.375	1.065	8.16 (4/26/12), FES3	1.099
20	B	Y	L1	37.5	0.375	0.935	4.8 (4/17/12), FES3	0.893
21	B	Y	L2	37.5	0.375	0.205	18.36 (5/25/12), FES1	0.305
22	T	N	L2	12.5	0.125	0.084	16.31 (5/23/12), FES1	0.163
23	T	N	L2	37.5	0.375	0.278	17.34 (5/24/12), FES3	0.178
24	T	Y	L2	12.5	0.375	0.14	19.38 (5/29/12), FES7	0.053
25	B	N	L2	12.5	0.125	0.097	17.33 (5/24/12), FES1	0.031
26	B	Y	L2	12.5	0.125	0.07	18.35 (5/25/12), FES1	-0.051
27	B	N	L2	12.5	0.375	0.202	16.32 (5/23/12), FES7	0.289
28	T	Y	L2	12.5	0.125	0.091	19.37 (5/29/12), FES1	0.199
29	T	N	N	12.5	0.375	0.164	20.39 (5/30/12), Retest of 11.22	0.179
30	B	N	N	12.5	0.125	0.415	10.19 (5/2/12), Replicate of 7.13	0.475
31	B	N	N	12.5	0.125	0.434	22.44 (6/1/12), Replicate of 7.13	0.475
32	B	N	N	12.5	0.125	0.431	23.46 (6/4/12), Replicate of 7.13	0.475
33	B	Y	N	12.5	0.125	0.366	11.21 (5/3/12), Replicate of 3.6	0.395
34	T	Y	N	12.5	0.125	0.105	12.23 (5/4/12), Replicate of 2.3, Anomaly	0.090
35	T	Y	N	12.5	0.125	0.113	20.40 (5/30/12), Replicate of 2.3	0.090
36	T	Y	N	37.5	0.375	0.275	23.45 (6/4/12), Replicate of 3.5	0.259
37	T	N	N	37.5	0.375	0.294	22.43 (6/1/12), Replicate of 7.14	0.377
38	B	Y	L1	12.5	0.125	0.294	13.25 (5/7/12), Replicate of 9.17	0.293
39	T	Y	L1	12.5	0.125	0.116	15.29 (5/10/12), Replicate of 8.15	0.150
40	T	N	L1	12.5	0.125	0.13	5.9 (4/19/12), Replicate of 4.7	0.082
41	B	N	L1	12.5	0.125	0.329	14.27 (5/9/12), Replicate of 6.11	0.343
42	B	N	L1	12.5	0.125	0.334	21.42 (5/31/12), Replicate of 6.11	0.343
43	T	N	L1	37.5	0.375	0.313	13.26 (5/7/12), Retest of 9.18, Anomaly	0.342
44	T	N	L1	37.5	0.375	0.307	21.41 (5/31/12), Retest of 9.18	0.342
45	B	N	N	25	0.25	0.921	CO.a (3/29/12), FES2, Check Out	0.885
46	B	N	N	12.5	0.25	0.797	CO.b (3/29/12), FES5, Check Out	0.731
47	T	N	N	12.5	0.125	0.129	1.1 (4/5/12), FES1, Non-DOE	0.052
48	B	N	L1	12.5	0.375	0.86	5.10 (4/19/12), FES7, Non-DOE	0.833

Appendix L.—Tabulated Delta Pressure for DOE and Supplementary Matrices

Pressure change data for both the DOE and Supplementary tests are tabulated in Table 14 with corresponding time durations which characterize time between ignition and the first time the pressure reaches its maximum for the run. Additional details are described below.

- t_peak is defined as the first time the pressure reaches a maximum value during the run. (Several cases show pressure reaching same maximum value more than once.)
- t_ignition is defined as the temperature at ignition. (Ignition can be determined from the raw data files as the time when column D, 1001<IGN_ACTIVE> (VDC), indicates its first non-zero reading.)
- Fill/Runs highlighted in red text indicate the following:
    - F11R22 experienced an anomaly and was excluded based on the t_peak value being 100 s larger than that on the retest F20R39.
    - F9R18 and F13R26 experienced anomalies that also affected t_peak and created a secondary decay in pressure as compared to retest F21R41.
    - Replicate F12R23 experienced an anomaly that had a minimal effect as compared to F2R3 and replicate F20R40 and was therefore included.

TABLE 14.—EXPERIMENTAL DELTA PRESSURE FOR DOE AND SUPPLEMENTARY TESTS

Fill(F)/Run(R)	P(t_peak) - P(t_ignition)	t_peak - t_ignition
DOE Tests		
F1R1	0.129	176
F1R2	1.369	9
F2R3	0.130	204
F2R4	1.051	25
F3R5	0.275	190
F3R6	0.394	10
F4R7	0.129	205
F4R8	0.935	9
F5R9	0.130	207
F5R10	0.860	28
F6R11	0.334	9
F6R12	0.281	193
F7R13	0.442	9
F7R14	0.337	169
F8R15	0.118	206
F8R16	1.065	10
F9R17	0.294	11
F9R18	0.315	107
F10R19	0.415	11
F10R20	0.149	744
F11R21	0.366	9
F11R22	0.161	709
F12R23	0.105	223
F12R24	0.859	26

F13R25	0.294	11
F13R26	0.313	172
F14R27	0.329	9
F14R28	0.759	27
F15R29	0.116	188
F15R30	0.164	677
F16R31	0.084	228
F16R32	0.202	83
F17R33	0.097	7
F17R34	0.278	242
F18R35	0.070	7
F18R36	0.205	8
F19R37	0.091	240
F19R38	0.140	752
F20R39	0.164	597
F20R40	0.113	203
F21R41	0.307	211
F21R42	0.334	9
F22R43	0.294	233
F22R44	0.434	9
F23R45	0.275	164
F23R46	0.431	9
Supplemental Tests		
F1R1	0.921	10
F1R2	0.797	17
F2R3	0.418	198
F3R4	1.293	20
F4R5	1.776	12
F5R6	1.611	28
F5R7		
F6R8	0.402	66
F6R9	1.280	78
F7R10	2.398	28
F7R11	0.704	29
F8R12	0.191	87
F8R13	0.592	56
F9R14	0.959	23
F10R15	0.706	38
F10R16	0.679	14
F11R17	0.326	8
F12R18	3.527	42
F13R19	0.541	17
F13R20	0.800	11
F14R21	2.719	30

Appendix M.—Stills From Test Video Files

The following still pictures (Figs. 49 to 55) were taken from the test video files. The various still pictures show tests with and without quench bars, top and bottom ignition, simultaneous and sequential burning, and cheesecloth and SIBAL material. The heat exchangers were mounted above the sample holders and were out of the field of view of the cameras. The video stills are all from the front cameras (the HDR-XR160 cameras).

Figure 49.—Three sample cheesecloth, bottom simultaneous ignition, with quench bars.

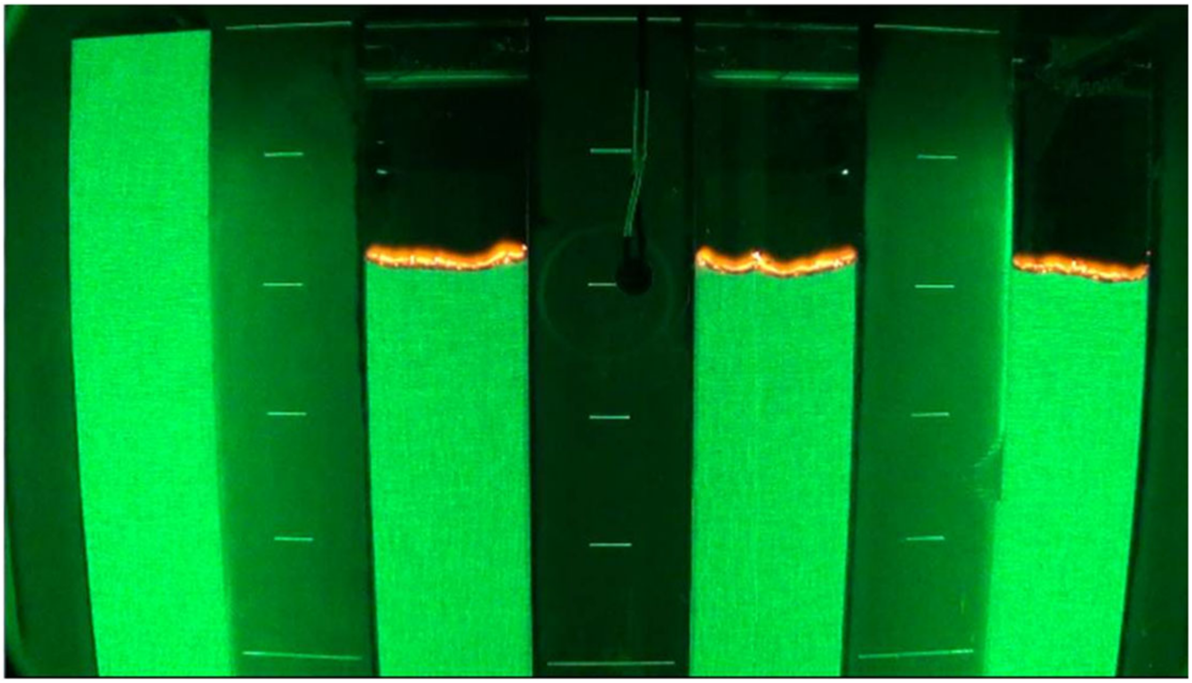

Figure 50.—Three sample cheesecloth, top simultaneous ignition, without quench bars.

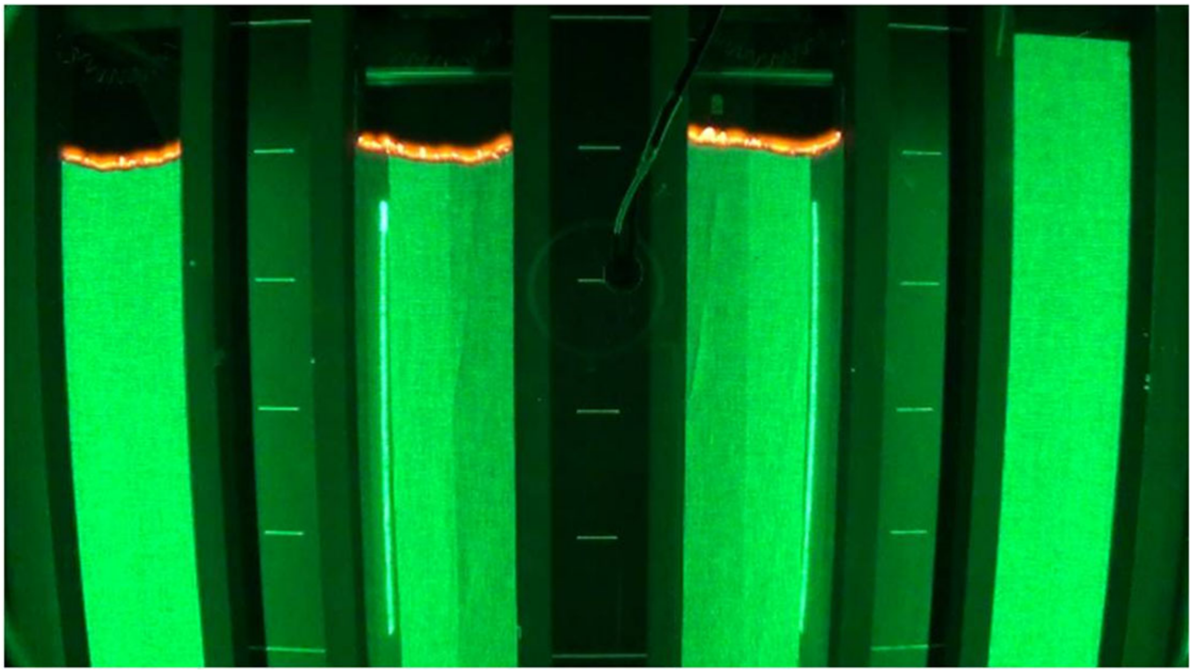

Figure 51.—Three sample cheesecloth, top simultaneous ignition, with quench bars.

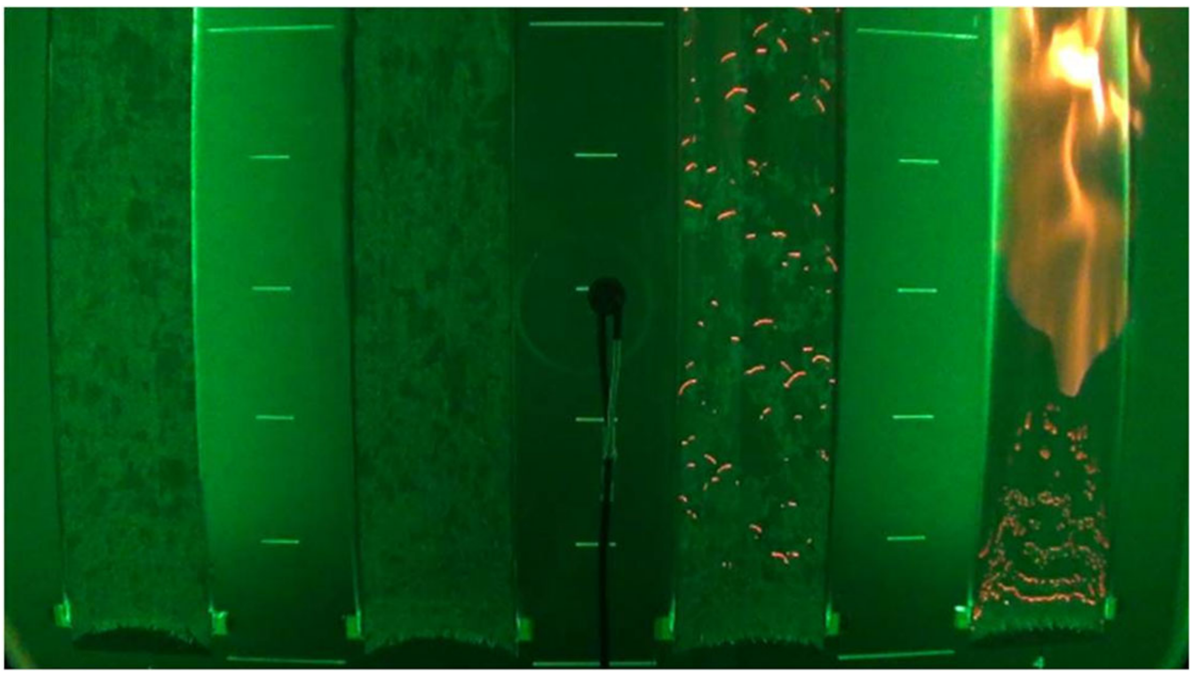

Figure 52.—Two sample SIBAL, bottom sequential ignition, without quench bars.